Spintronic Interface design

(スピントロニクス・インターフェース・デザイン)

Yoshio Miura

Kyoto Institute of Technology (KIT)

Topics

Spintronic Interface design

1. Introduction on spintronics

2. Spin-dependent transport in magnetic tunnel junctions with half-metallic Heusler alloys

Y. Miura, *et al*., PRB **83,** 214411 (2011).

K. Masuda, T. Tadano, Y. Miura, PRB **104**, L180403 (2021).

3. First-Principles Study on magnetic damping of Fe(001) interface

R. Mandal, et al., Phys. Rev. Applied **14**, 064027 (2020).

Introduction of spintronics

What is spintronics?

Electronics utilizing not only charge of electrons but also spin of electrons, simultaneously.

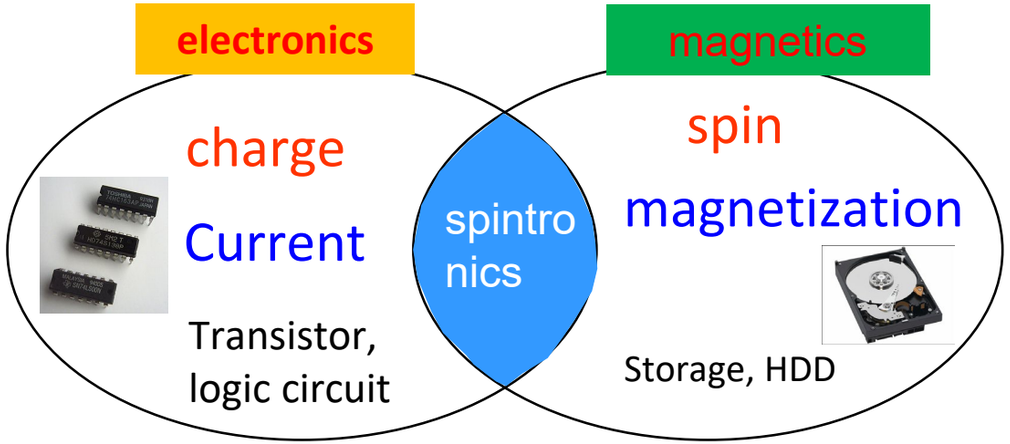

Magneto-resistive devices

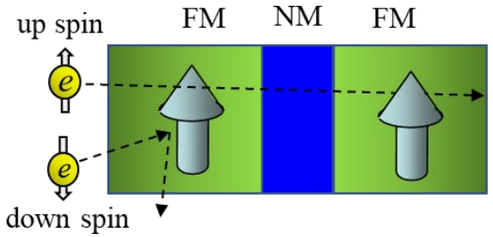

Parallel magnetization

R_P : small

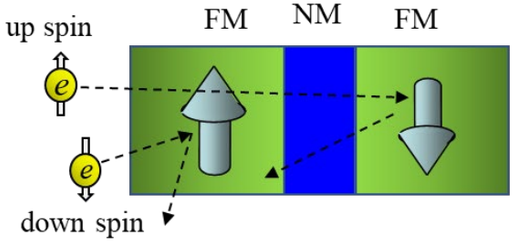

Anti-parallel magnetization

R_{AP} : large

(Tunnel) Magnetoresistance ((T)MR) effect

$$(\mathrm{T})\mathrm{MR\ ratio} = \frac{R_{AP} - R_P}{R_{AP}} \times 100$$

Tunnel→Non-Magnetic Insulator

Electronic structures

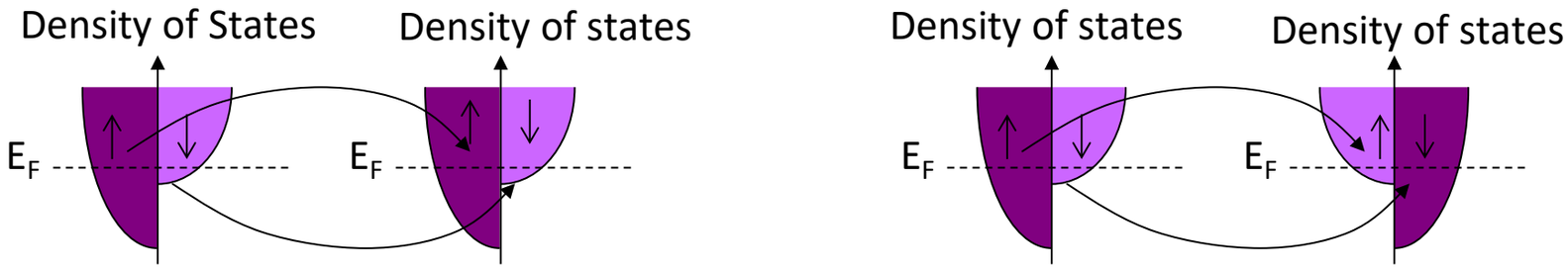

Conductivity : $G_P = D_L^{\uparrow} \cdot D_R^{\uparrow} + D_L^{\downarrow} \cdot D_R^{\downarrow}$ > $G_{AP} = D_L^{\uparrow} \cdot D_R^{\downarrow} + D_L^{\downarrow} \cdot D_R^{\uparrow}$

Read-out head of Hard Disk Drive (HDD)

Structure of HDD

Read-out head

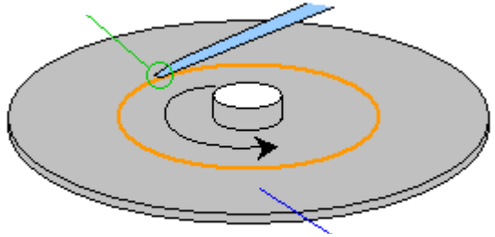

Storage media
(Magnetic thin film)

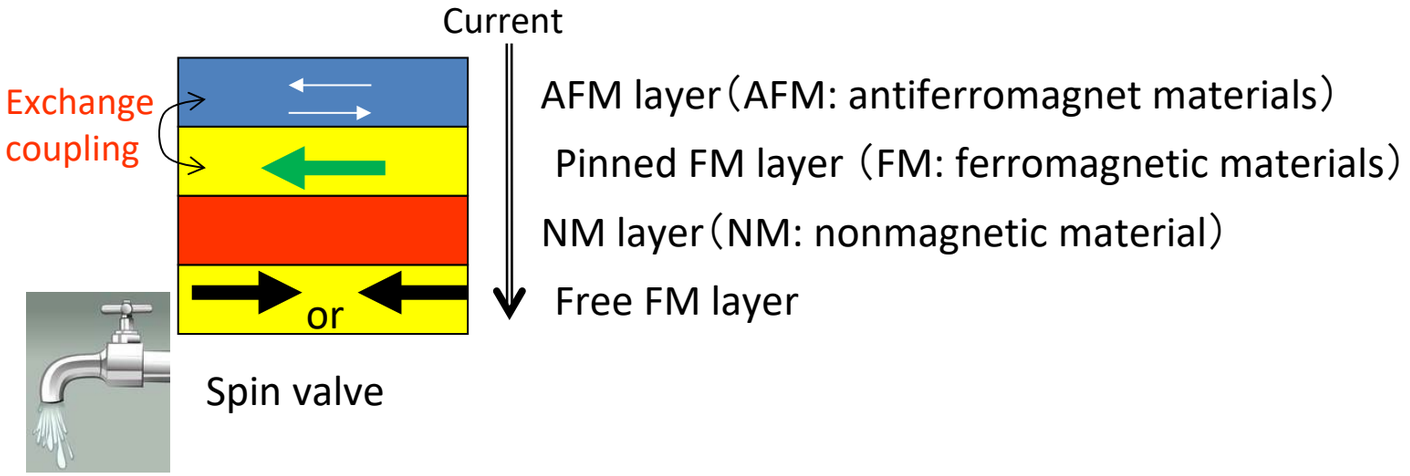

Structure of read-out head

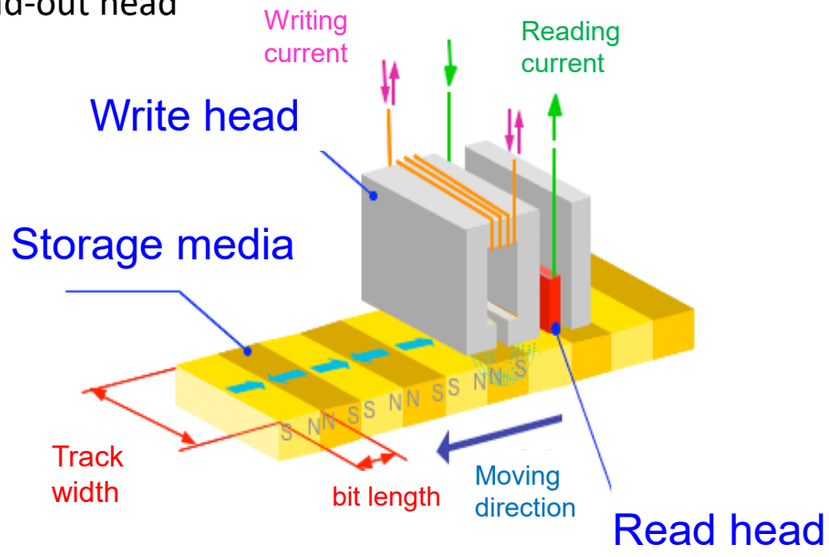

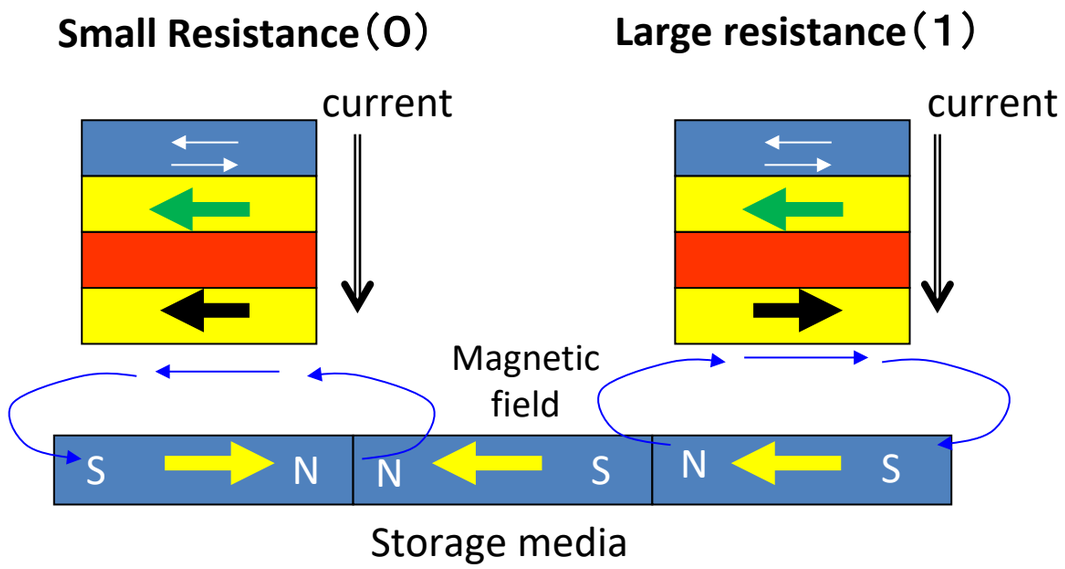

From press release of AIST

Spintronics application

Magneto-resistive sensor


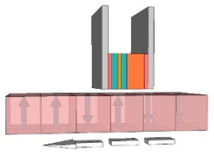

HDD read-out-head



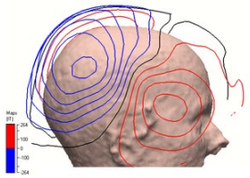

Earth's magnetic field sensor・current sensor for car・biomagnetic sensor

Corresponding to SQUID

Magneto-resistive Random Access Memory (MRAM)

・Non volatile memory
・Fast writing speed (10～50ns)
・Low electricity consumption (～30μW)
・Long endurance (10 years)

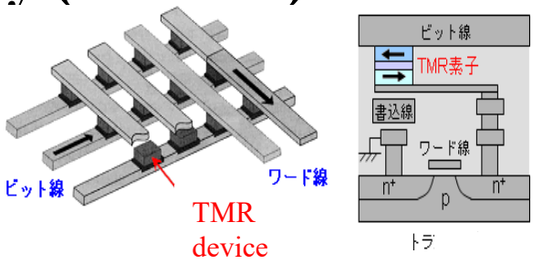

Everspin
64Mbit MRAM

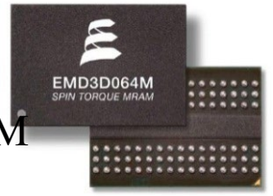

SRAM(Static RAM)⇒MRAM for non-volatile cash and core memory

Comparison of performance of non-volatile memory

Nanotechology 31, 092001 (2020).

	RRAM	PCM	MRAM	FeRAM
ON/OFF Ratio	20–50	10^2–10^4	1.5–2	10^2–10^3
Endurance	10^5–10^8	10^6–10^9	$> 10^{12}$	10^{10}
Retention	Medium	Large	Medium	Large
Drift	Weak	Yes	No	No
Linearity	Low	Low	None	None
Integration density	High	High	High	Low
Energy efficiency	0.1–1 pJ/bit	10 pJ/bit	100 fJ/bit	100 fJ/bit
Switching speed	<10 ns	10–100 ns	<10 ns	30 ns

Future Task

Large ON/OFF ratio (Magneto-resistance)

Low energy consumption in switching

RRAM: Resistive switching random access memory
PCM: Phase change memory
FeRAM: Ferroelectric random access memory

Magnetization reversal in Magnetic Tunnel Junctions (MTJs)

1. Magnetic field by current

problem：・complicate circuit.

・current∝1/device-size

Effects of demagnetizing field increase the critical current for writing with decreasing size of device

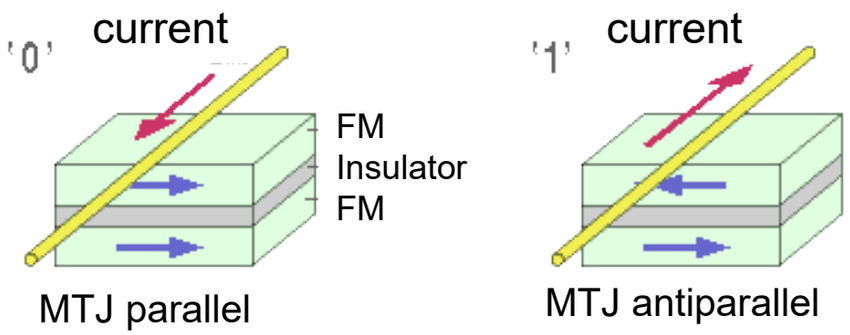

2. Spin transfer torque（STT）

The spin flip of conductive electron give the torque to the local spin moment due to the angular momentum conservation

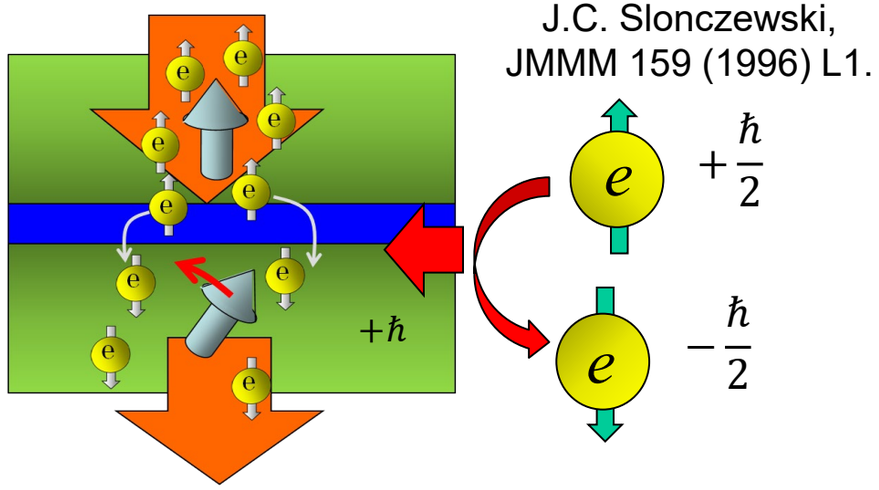

J.C. Slonczewski, JMMM 159 (1996) L1.

STT MRAM

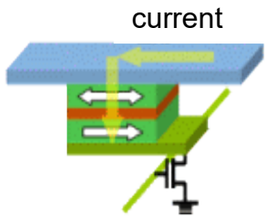

conventional MRAM

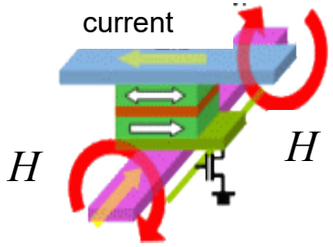

・simple circuit

・current∝device-size

Tohoku Univ. Ando lab. HP

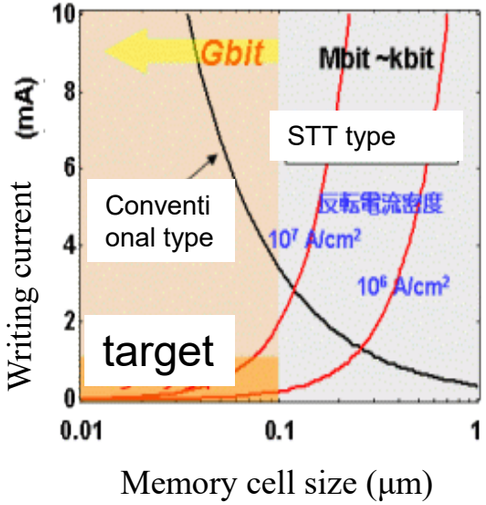

Magnetization reversal by spin transfer torque (STT)

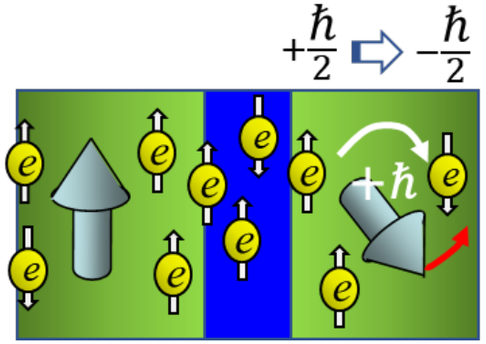

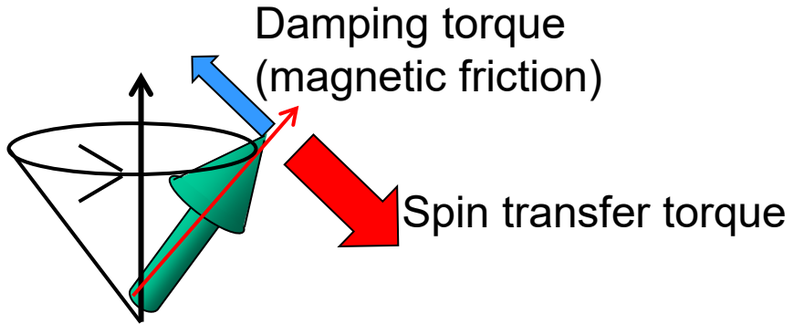

Reduction of critical current density (J_{c0})

$(10^7 \mathrm{A/cm^2} \Rightarrow 10^5 \mathrm{A/cm^2})$

$$J_{c0} \propto \alpha M_S [H_{\mathrm{anti}} \pm 4\pi M_S]\ t/P$$

J.C. Slonczewski, JMMM 159 (1996) L1.

α : Magnetic damping constant
M_S : Saturation Magnetization
$H_{\mathrm{anti}} \pm 4\pi M_S$: Effective anisotropy field
P : Spin polarization of current
t : Thickness of FM layer

1. High spin polarization (P) of current

2. Perpendicular magnetic anisotropy(PMA) H_{anti}-$4\pi M_s$

3. Low damping constant(α)

Large tunnel magneto-resistance (TMR) in magnetic tunnel junctions (MTJs)

Development of barrier layer
is very important!

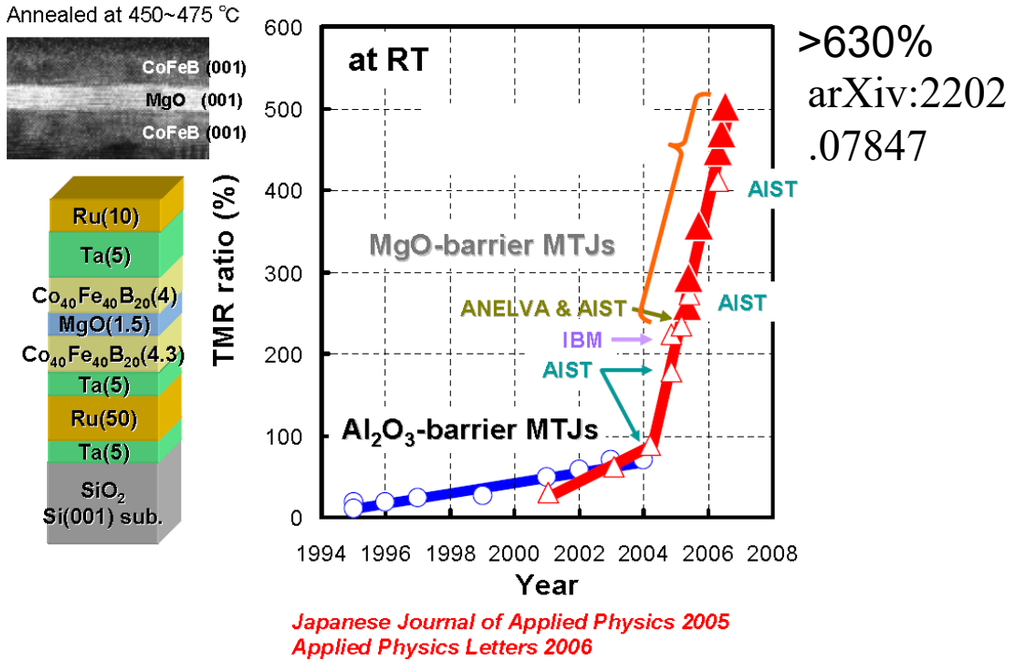

Amorphous Al-O barrier MTJ

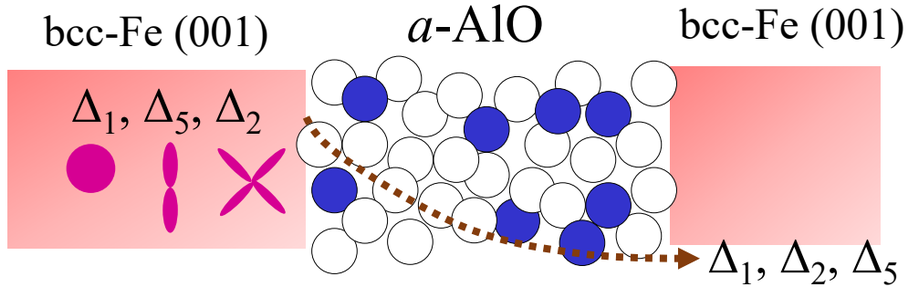

Crystalline-MgO barrier MTJ

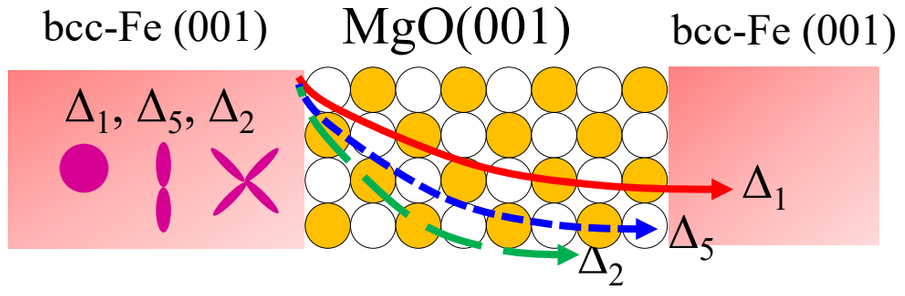

W. H. Butler, *et al.*, PRB **63**, 054416 (2001).

Bcc-Fe
⇒half-metallic on Δ_1 state

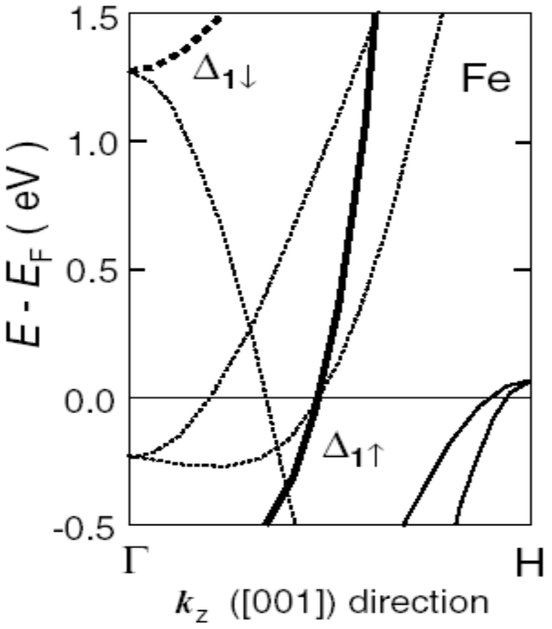

Now, Fe/MgO/Fe(001) MTJs have been used as a read-out-head of HDD!

Why the Δ_1 state show the slowest decay in MgO barrier?

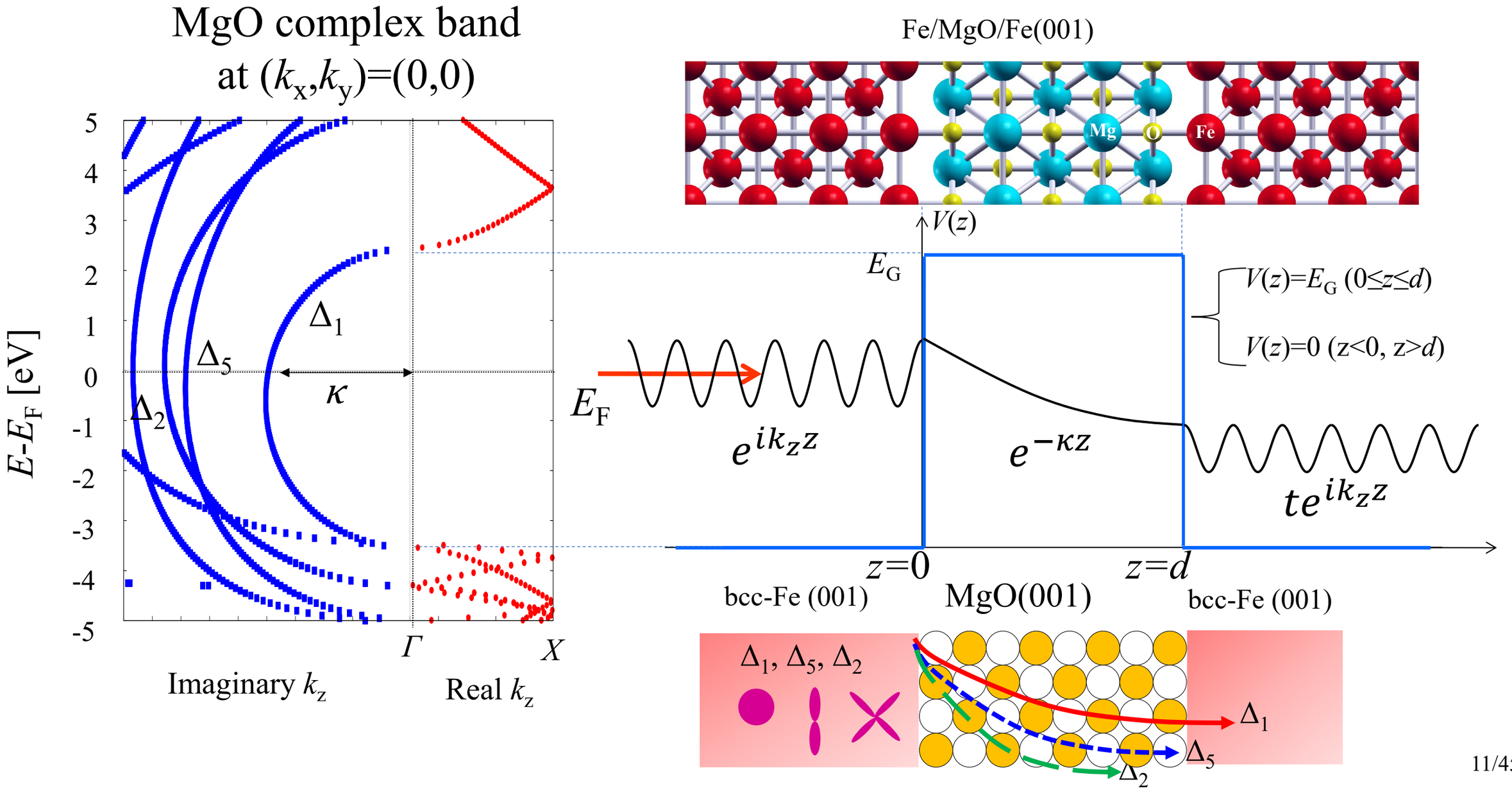

Why Fe/MgO/Fe(001) MTJs show the larger TMR?

Fe band and transmittance in Fe/MgO/Fe(001) at $(k_x,k_y)=(0,0)$

(Parallel magnetization)

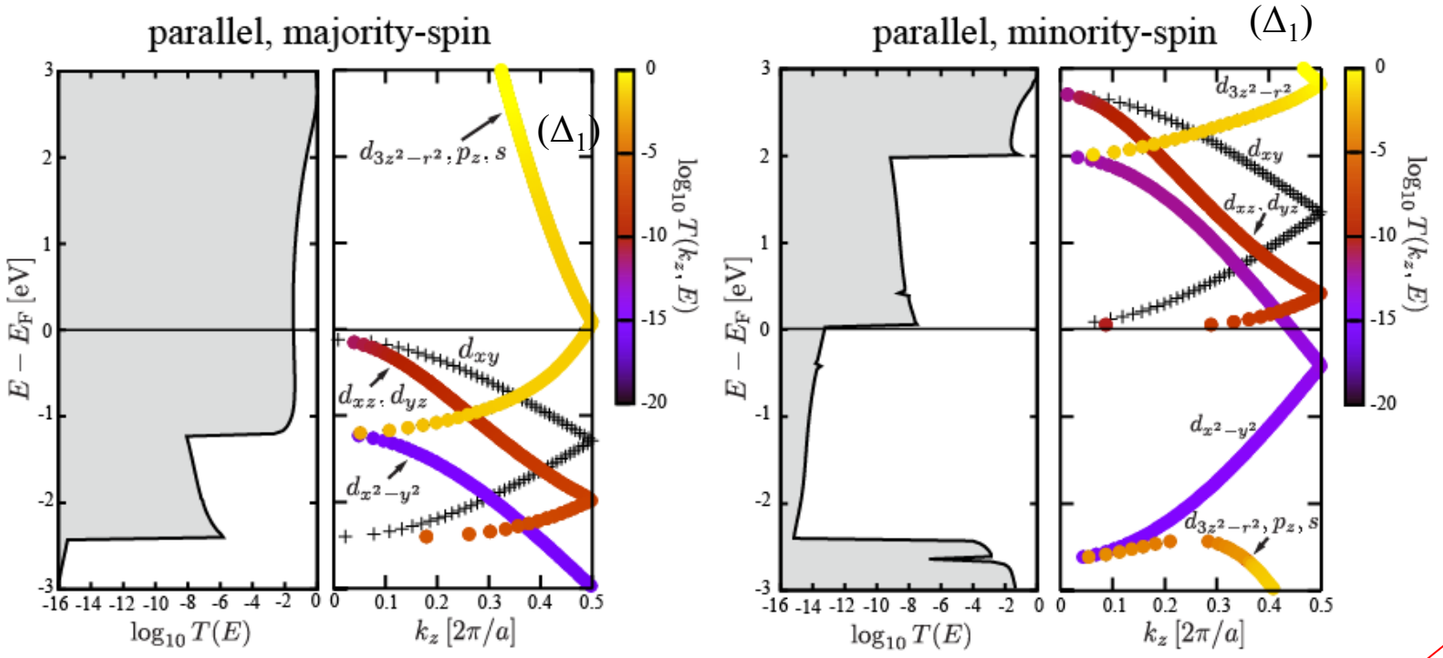

k-parallel (k_x,k_y) dependence of transmittance at E_F of Fe/MgO/Fe(001)

Majority-spin

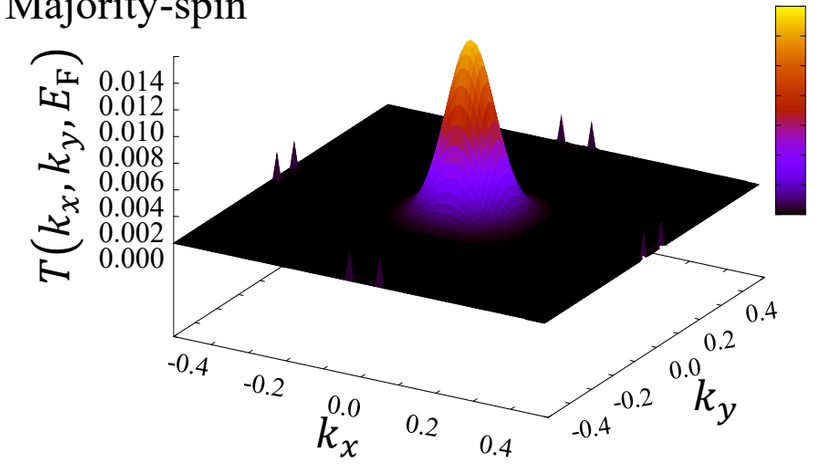

Minority-spin

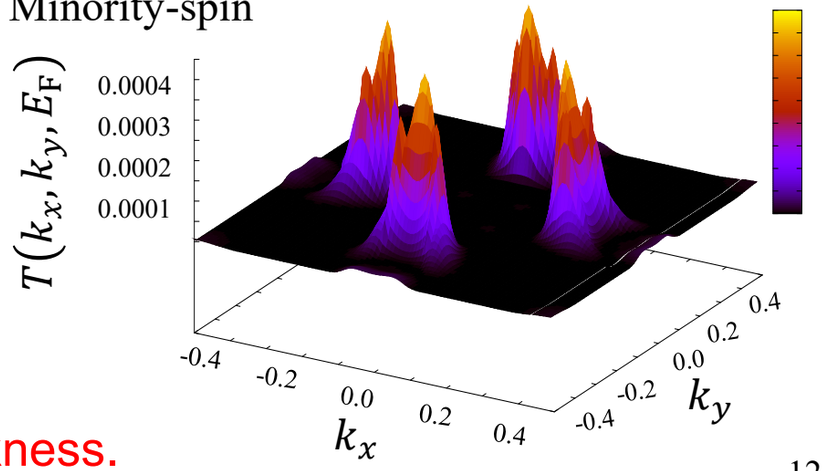

TMR ratio of Fe/MgO/Fe(001) MTJ is around 3000% for 2nm MgO thickness.

Topics

1. Introduction on spintronics

2. Spin-dependent transport in magnetic tunnel junctions with half-metallic Heusler alloys

Y. Miura, *et al*., PRB **83,** 214411 (2011).

K. Masuda, T. Tadano, Y. Miura, PRB **104**, L180403 (2021).

3. First-Principles Study on magnetic damping of Fe(001) interface

R. Mandal, et al., Phys. Rev. Applied **14**, 064027 (2020).

Introduction: Half-metallic ferromagnets

Julliere model

$$TMR = \frac{G_P - G_{AP}}{G_P} = \frac{2P_L \cdot P_R}{1 - P_L \cdot P_R}$$

Spin-polarization at E_F $\quad P_{L(R)} = \frac{D^{\uparrow}_{L(R)} - D^{\downarrow}_{L(R)}}{D^{\uparrow}_{L(R)} + D^{\downarrow}_{L(R)}}$

The Half-metallic ferromagnets

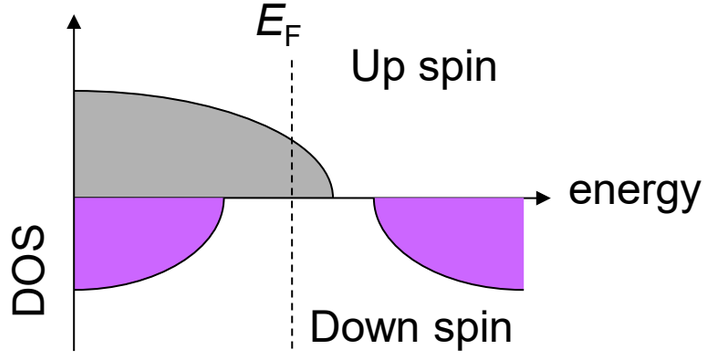

Co-based full Heusler alloys Co_2YZ (Y=Fe,Mn,Cr : Z=Si,Ge,Al,Ga)

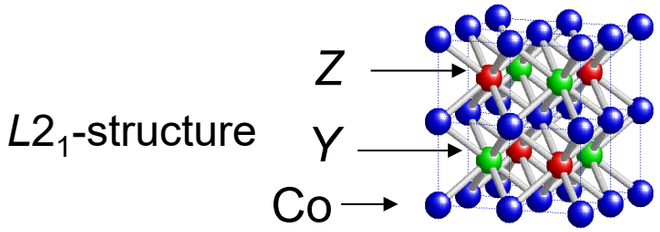

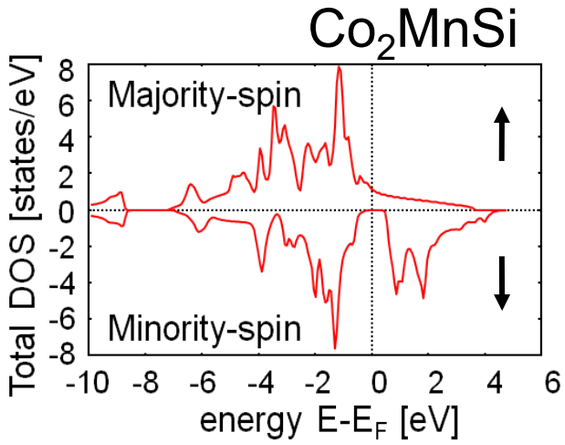

(1) B2-type disorder

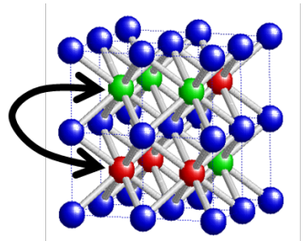

$Co_2(Mn_{1-y}Si_y)(Si_{1-y}Mn_y)$

(2) D03-type disorder

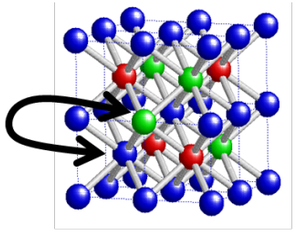

$(Co_{2-y}Mn_y)(Mn_{1-y}Co_y)Si$

High Curie temperature (900K)

Simple fabrication process

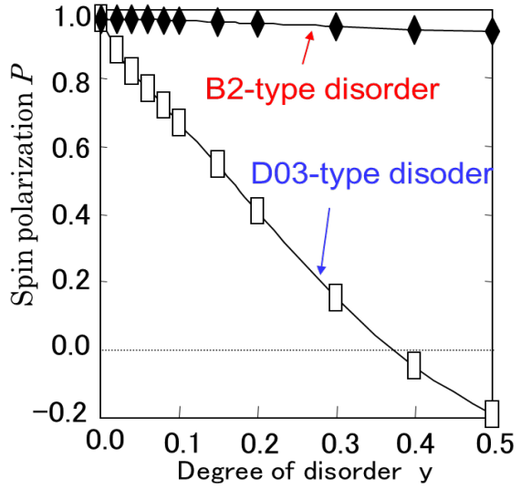

Y. Miura, *et al.*, PRB, 69 (2004) 144413.

Problem in MTJs with half-metallic Heusler alloys

Experiment

TMR ratio of MTJs with Co_2MnSi(CMS)

CMS/AlO/CMS

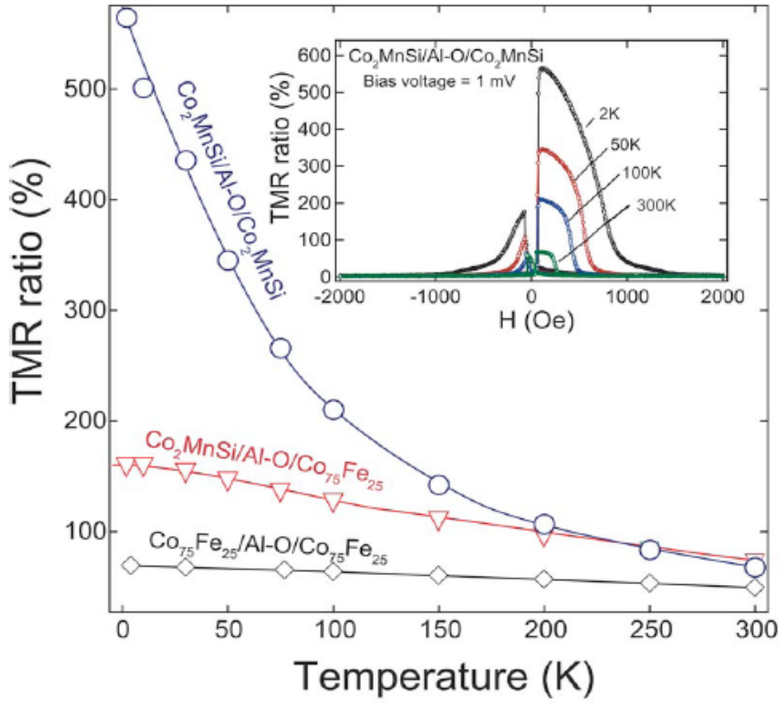

Y. Sakuraba, *et al*., Appl. Phys. Lett. **88,** 192508 **(**2006).

Top data

CMS/MgO/CMS(001)

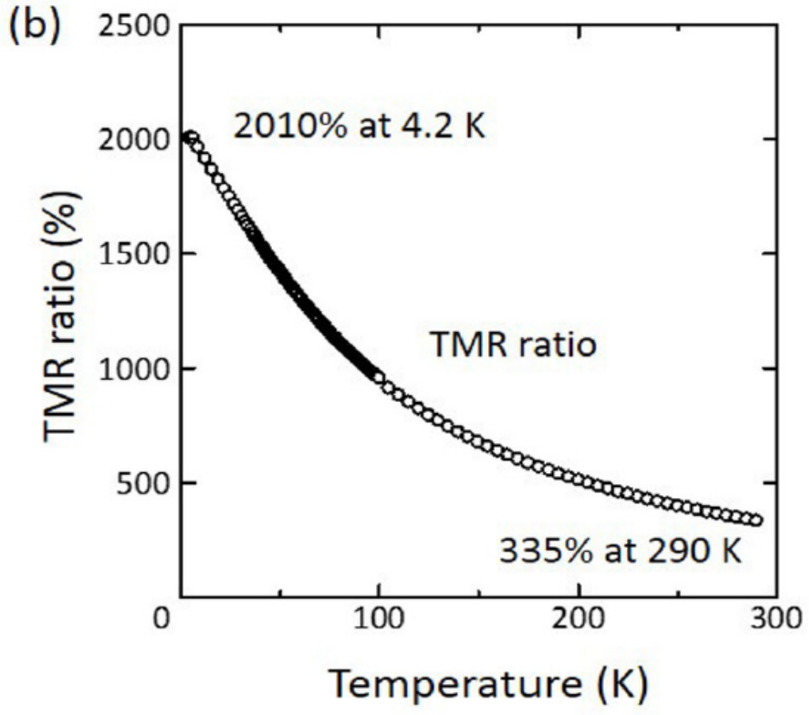

B. Hu, et al., PRB **94** (2016) 094428.

Problem: Reduction of the TMR ratio at room temperature

in spite of high curie temperature of Co_2MnSi: 985K

Problem in MTJs with half-metallic Heusler alloys

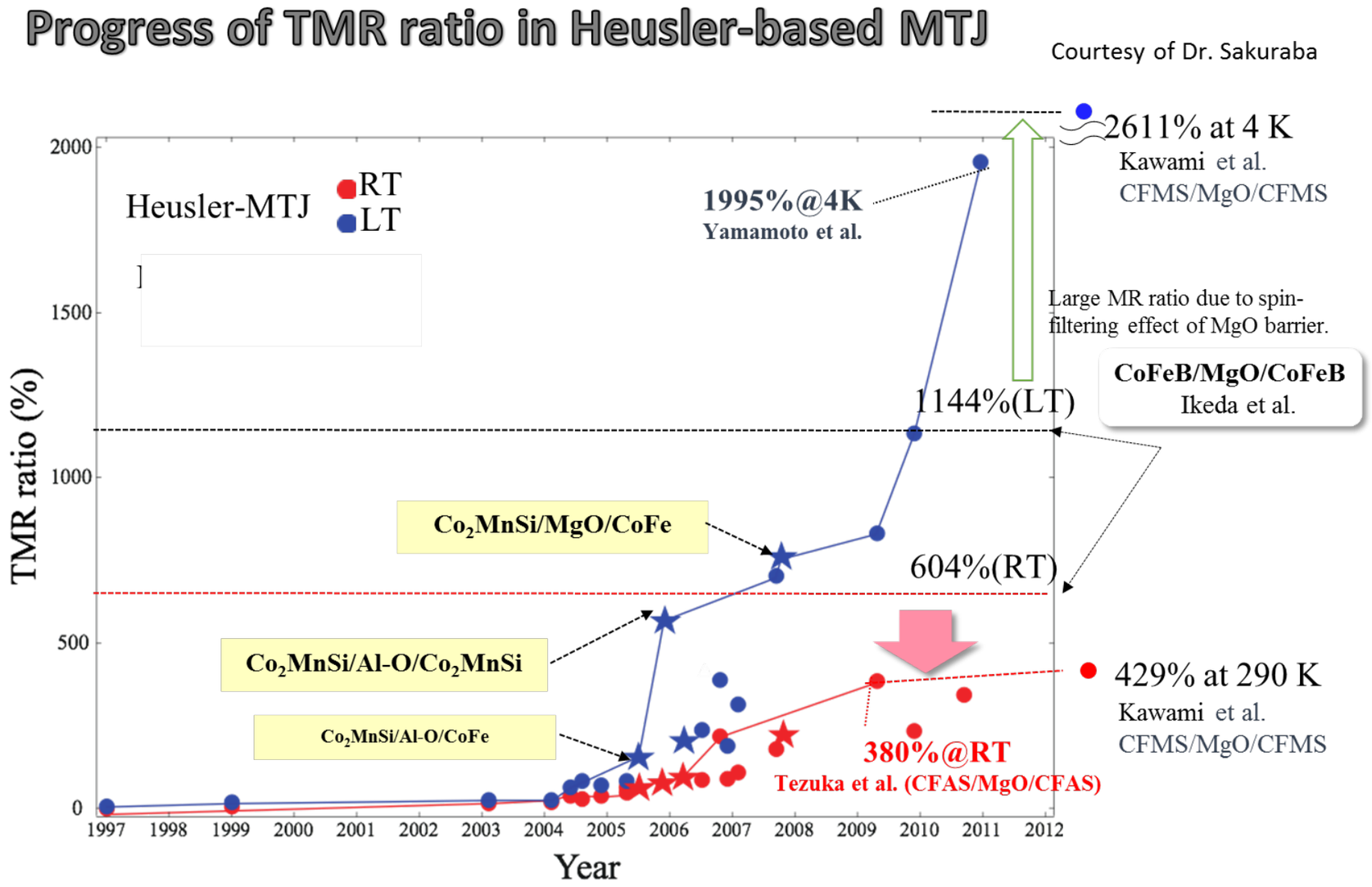

Heusler-based MTJ : Large temperature dependence of MR ratio is still a serious problem especially in CMS.

CMS: Co_2MnSi CFAS: $Co_2Fe(AlSi)$ CFMS: $Co_2(FeMn)Si$

Theoretical consideration

1. Temperature dependence of bulk density of states

Spin resolved hard X-ray photoemission of Co_2MnSi thin film

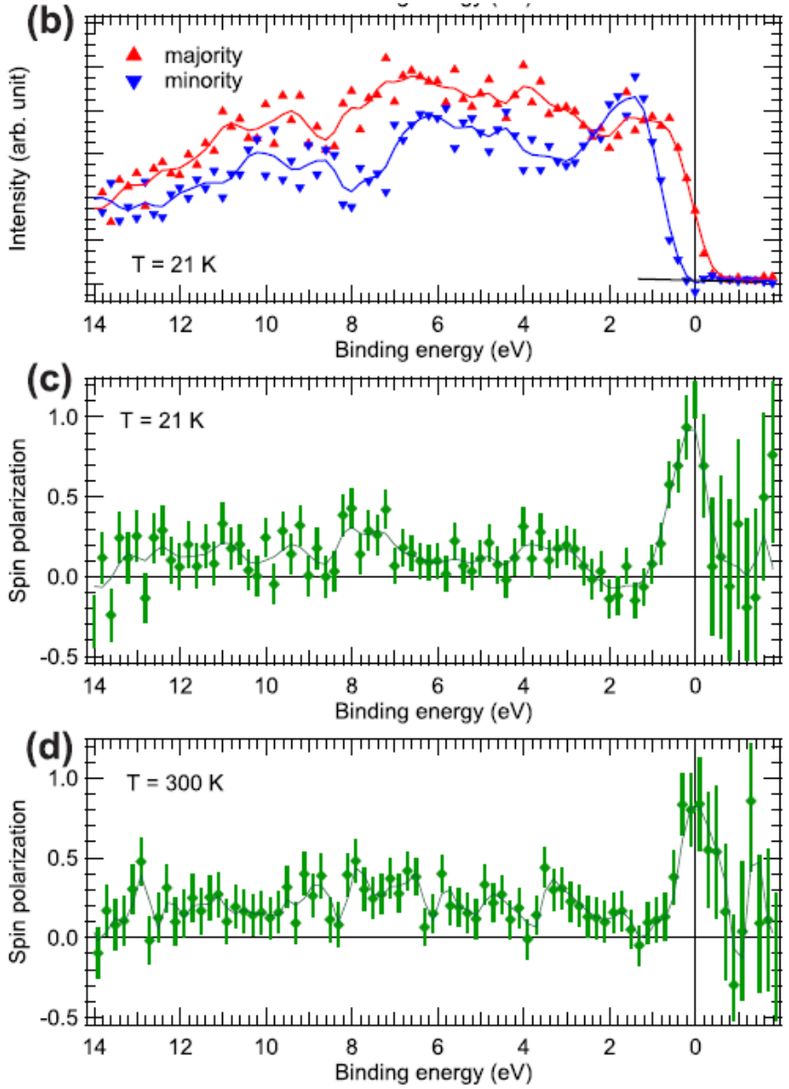

S. Ueda, et al., PRB **106**, 075101 (2022)

High spin polarization hardly reduce at 300K.

Disordered Local Moment (DLM) method

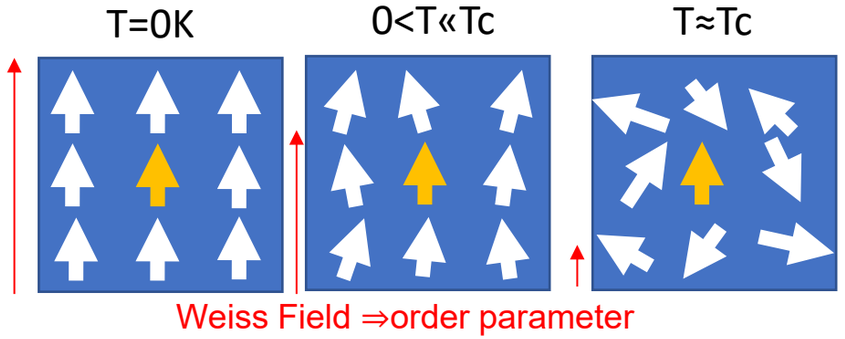

Temperature dependence of total DOS of bulk CMS calculated from DLM

K. Nawa, *et al*., PRB 102, 054424 (2020).

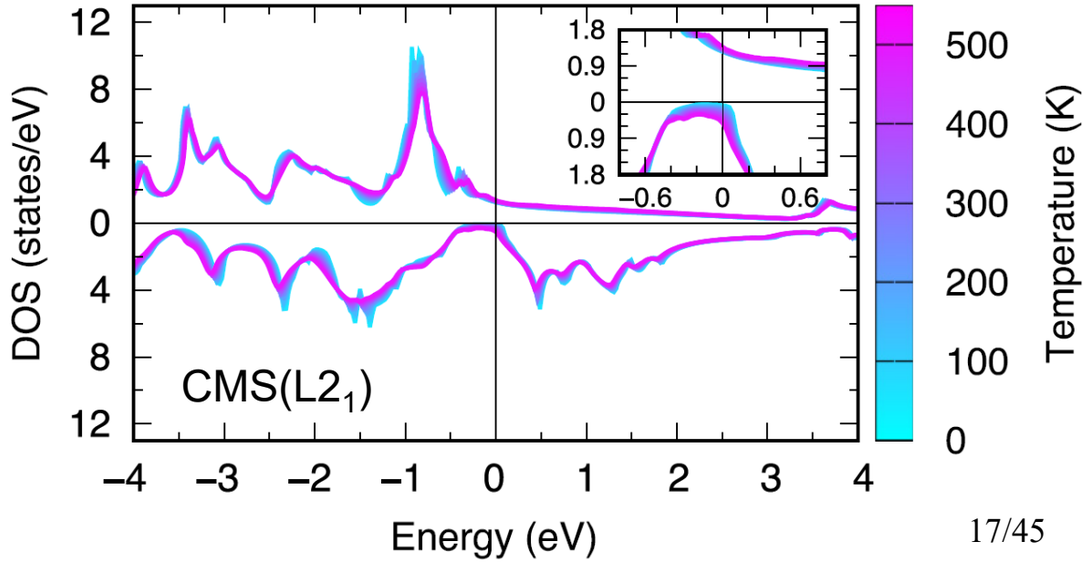

Theoretical consideration

2. Effects of the spin-flip scattering through the interface states promoted by magnetic excitation.

P. Mavropoulos, *et al*., PRB, 72 (2005) 174428.

Anti-parallel magnetization

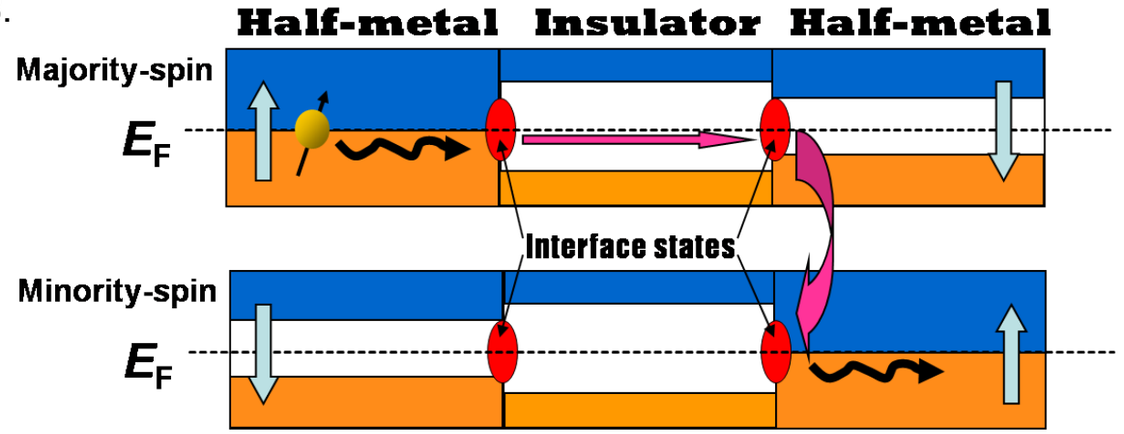

$Co_2MnSi/MgO(001)$

Y. Miura, *et al*., PRB 78, 064416 (2008).

Y. Miura, *et al*., JPCM 19, 365228 (2007).

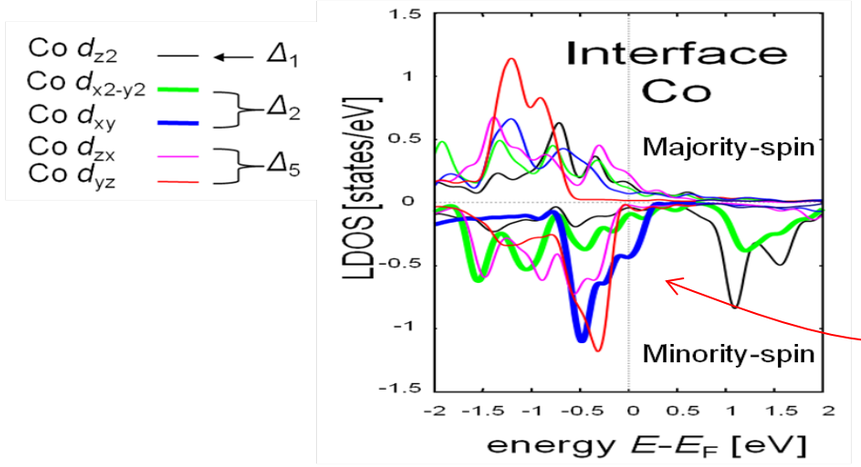

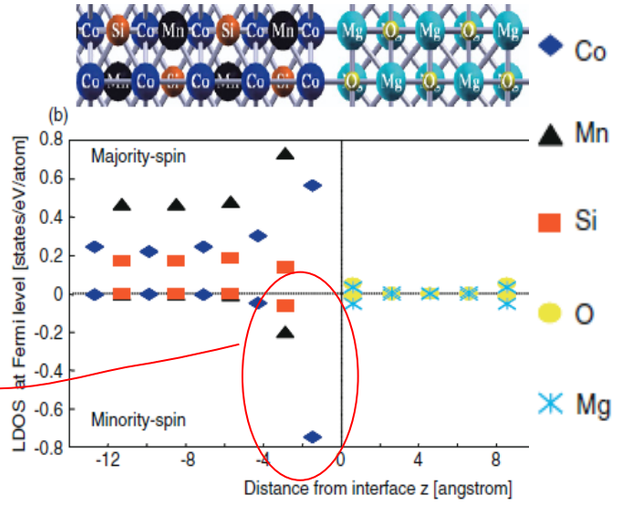

How we can treat interfacial effects in TMR

Conductance calculation in Non-collinear spin system

First, we perform electronic structure calculations in collinear spin system

Then, we artificially rotate spin-quantum axis of local spin-moments to obtain density-matrix in non-collinear spin system.

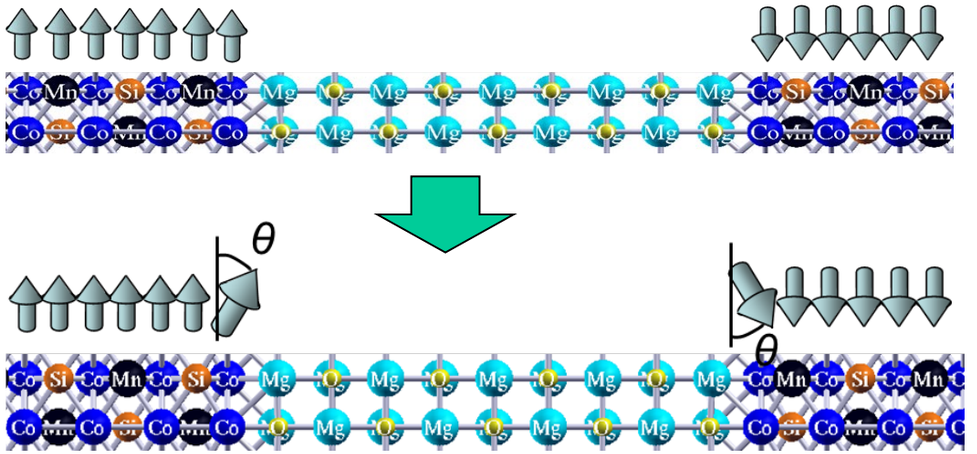

Electronic structures http://www.pwscf.org/

- Plane-wave basis set
- Ultra-soft pseudopotential method
- GGA for Exchange-Correlation term

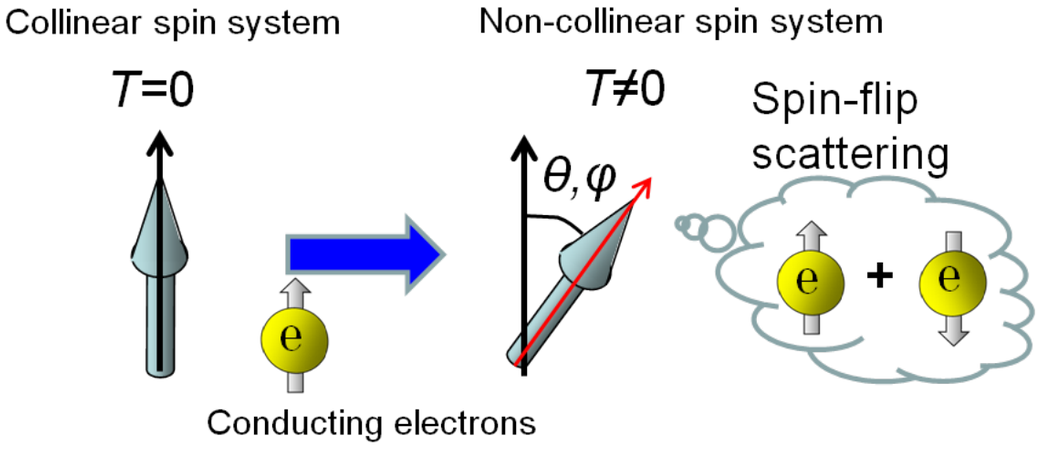

Transport calculations A. Smogunov, et al., PRB **70**, (2004) 045417.

$$G = \frac{e^2}{h}\sum_{i}^{N} T_i$$

- Landauer formula
- Zero bias limet Ballistic Conductance

The rotation of spin-quantum axis in NC spin system

The density matrix in non-collinear spin system is obtained from the inverse unitary transformation of spin-density in collinear spin system.

Collinear spin system($\mathbf{n}_i$) Non-collinear spin system($\mathbf{n}_{\alpha\beta}$)

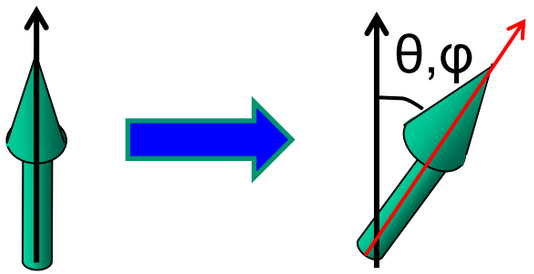

$$\sum_{\alpha\beta} U_{i\alpha}(\mathrm{r})\, n_{\alpha\beta}(\mathrm{r}) U^{+}_{\beta j} = \delta_{ij} n_i(\mathrm{r})$$

$$U = \begin{pmatrix} \exp\left(\frac{1}{2}i\phi\right)\cos\left(\frac{1}{2}\theta\right) & \exp\left(-\frac{1}{2}i\phi\right)\sin\left(\frac{1}{2}\theta\right) \\ -\exp\left(\frac{1}{2}i\phi\right)\sin\left(\frac{1}{2}\theta\right) & \exp\left(-\frac{1}{2}i\phi\right)\cos\left(\frac{1}{2}\theta\right) \end{pmatrix}$$

J. Kubler et al., J. Phys. F: Met. Phys. **18**, 469 (1988).

Local potential in Collinear spin system

$$\begin{pmatrix} V_L(r) + V_H(r) + \frac{1}{2}\sum_{\alpha=(\uparrow,\downarrow)} \frac{\delta E_{XC}}{\delta n_\alpha} + \frac{1}{2}\left(\frac{\delta E_{XC}}{\delta n_\uparrow} - \frac{\delta E_{XC}}{\delta n_\downarrow}\right) & 0 \\ 0 & V_L(r) + V_H(r) + \frac{1}{2}\sum_{\alpha=(\uparrow,\downarrow)} \frac{\delta E_{XC}}{\delta n_\alpha} - \frac{1}{2}\left(\frac{\delta E_{XC}}{\delta n_\uparrow} - \frac{\delta E_{XC}}{\delta n_\downarrow}\right) \end{pmatrix}$$

Local potential in Non-Collinear spin system

$$\begin{pmatrix} V_L(r) + V_H(r) + \frac{1}{2}\sum_{\alpha=(\uparrow,\downarrow)} \frac{\delta E_{XC}}{\delta n_\alpha} + \frac{1}{2}\left(\frac{\delta E_{XC}}{\delta n_\uparrow} - \frac{\delta E_{XC}}{\delta n_\downarrow}\right)\cos\theta & \frac{1}{2}\left(\frac{\delta E_{XC}}{\delta n_\uparrow} - \frac{\delta E_{XC}}{\delta n_\downarrow}\right)\sin\theta\cos\varphi + \frac{i}{2}\left(\frac{\delta E_{XC}}{\delta n_\uparrow} - \frac{\delta E_{XC}}{\delta n_\downarrow}\right)\sin\theta\sin\varphi \\ \frac{1}{2}\left(\frac{\delta E_{XC}}{\delta n_\uparrow} - \frac{\delta E_{XC}}{\delta n_\downarrow}\right)\sin\theta\cos\varphi - \frac{i}{2}\left(\frac{\delta E_{XC}}{\delta n_\uparrow} - \frac{\delta E_{XC}}{\delta n_\downarrow}\right)\sin\theta\sin\varphi & V_L(r) + V_H(r) + \frac{1}{2}\sum_{\alpha=(\uparrow,\downarrow)} \frac{\delta E_{XC}}{\delta n_\alpha} - \frac{1}{2}\left(\frac{\delta E_{XC}}{\delta n_\uparrow} - \frac{\delta E_{XC}}{\delta n_\downarrow}\right)\cos\theta \end{pmatrix}$$

Y. Miura, et al., Phys. Rev. B **83,** 214411 (2011).

Transport in non-collinear spin MTJs

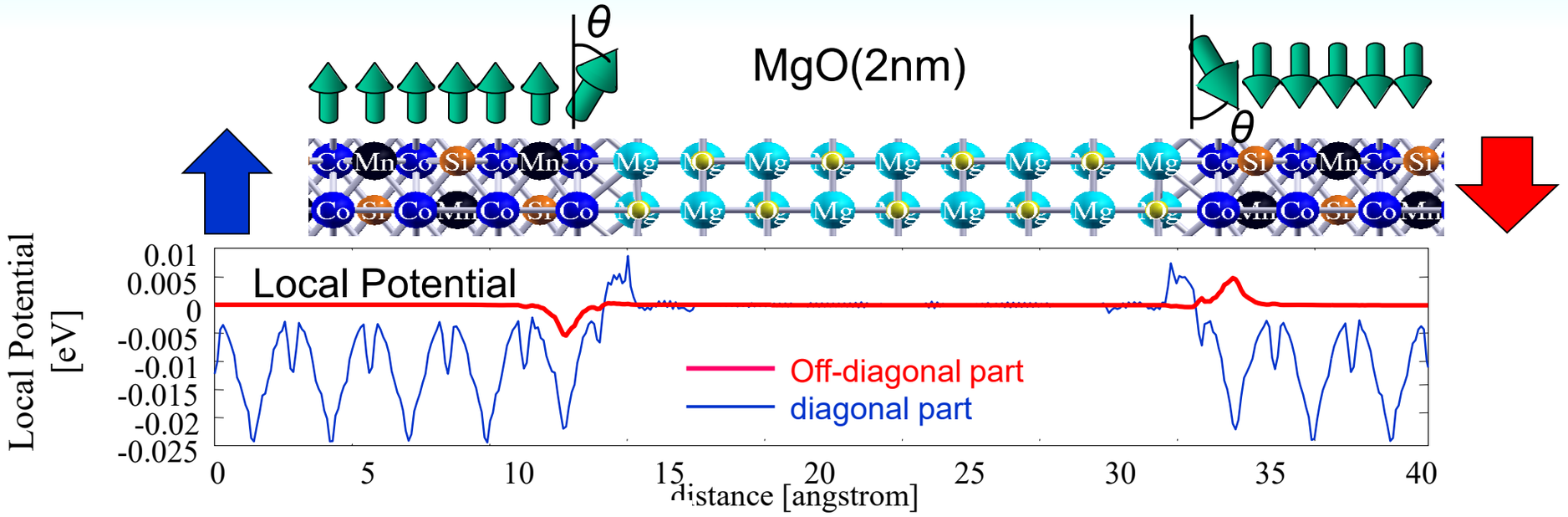

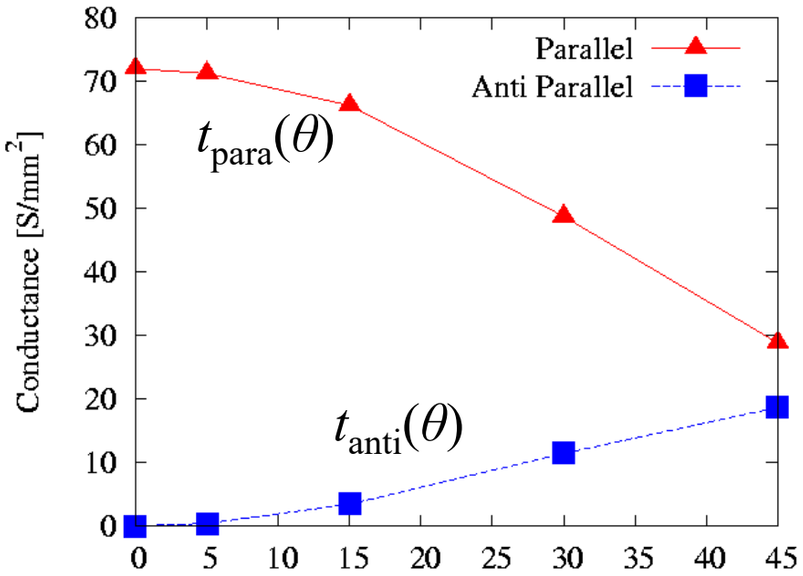

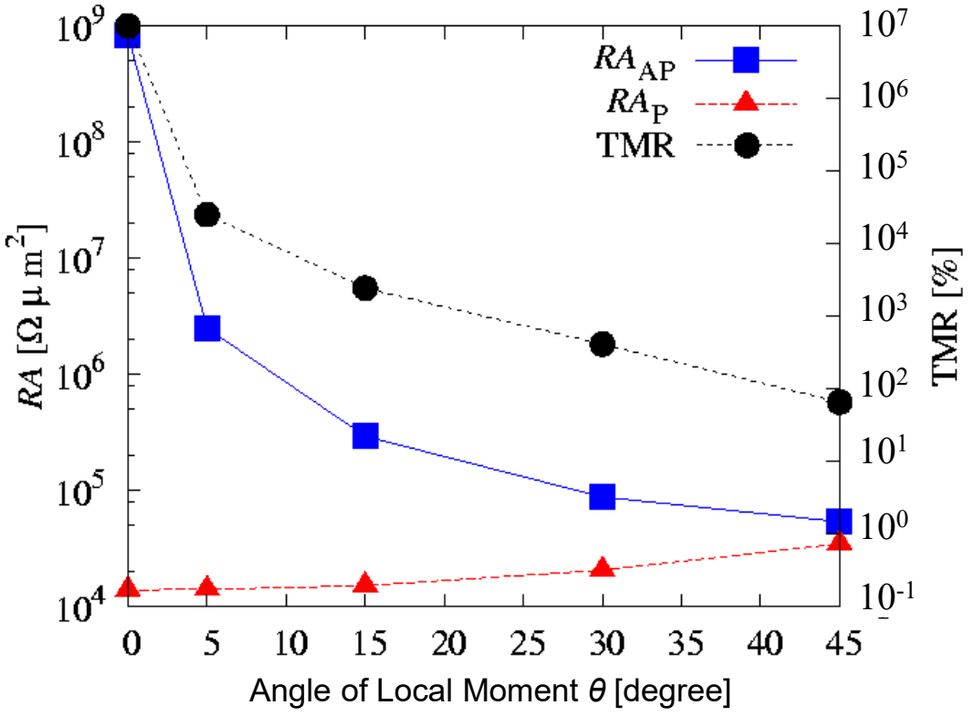

Y. Miura, et al., Phys. Rev. B **83,** 214411 (2011).

$k_{//}$-dependence of spin-flip conductance

Co_2MnSi(Zv=29)

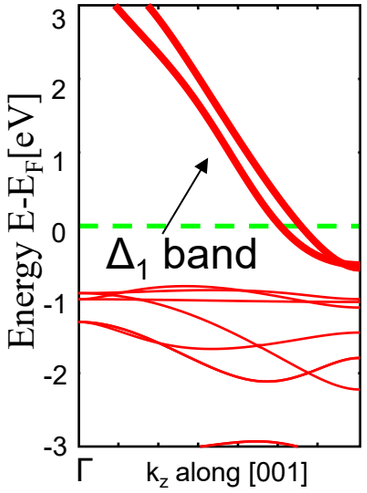

MgO 9-layer（thickness～2nm)

Parallel magnetization
(θ=15°,φ=0°)

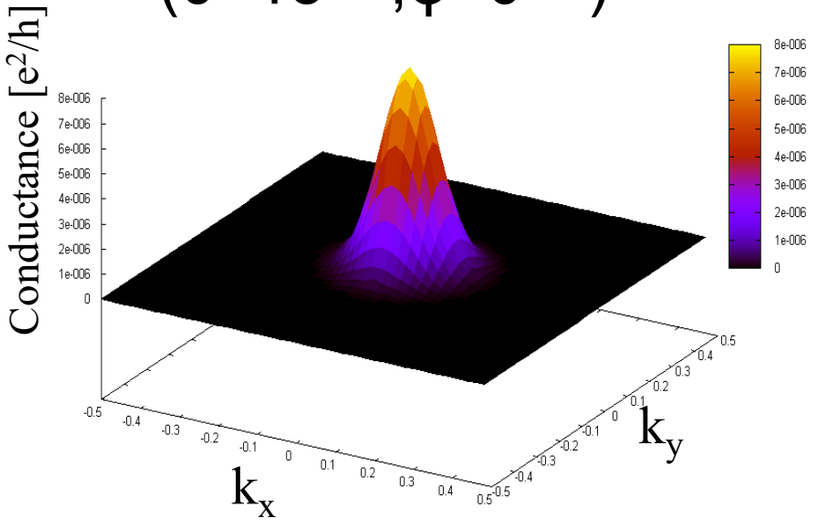

Anti-parallel magnetization
(θ=15°,φ=0°)

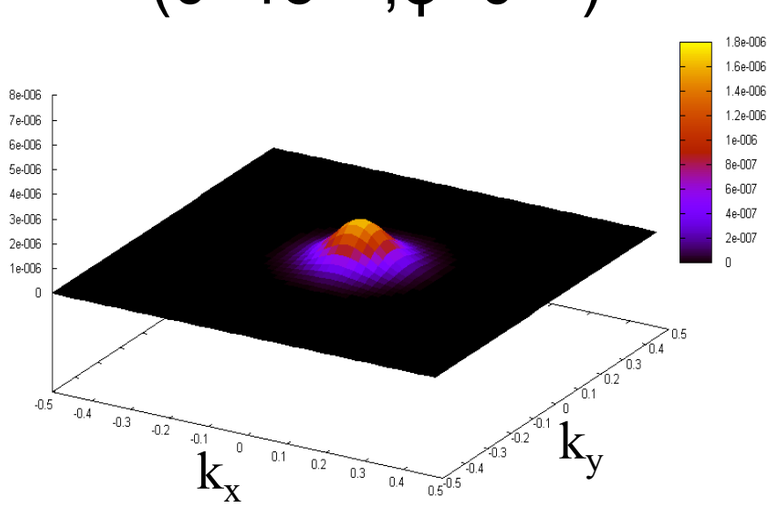

Spin-flip conductance in anti-parallel magnetization is dominated by the Δ_1 tunneling states.

LDOS image at interfaces

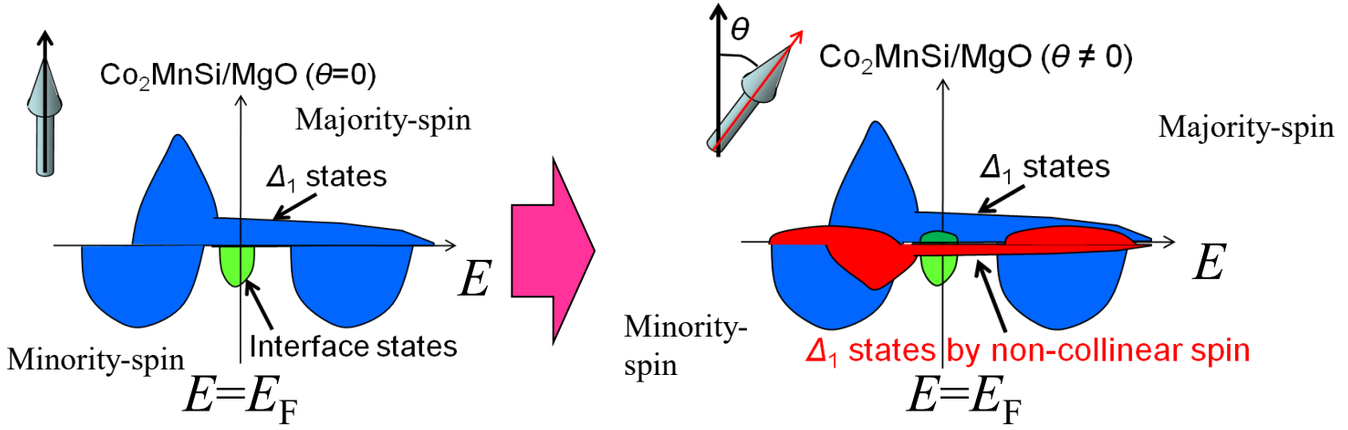

Effects of sub-interfacial non-collinear spin to TMR

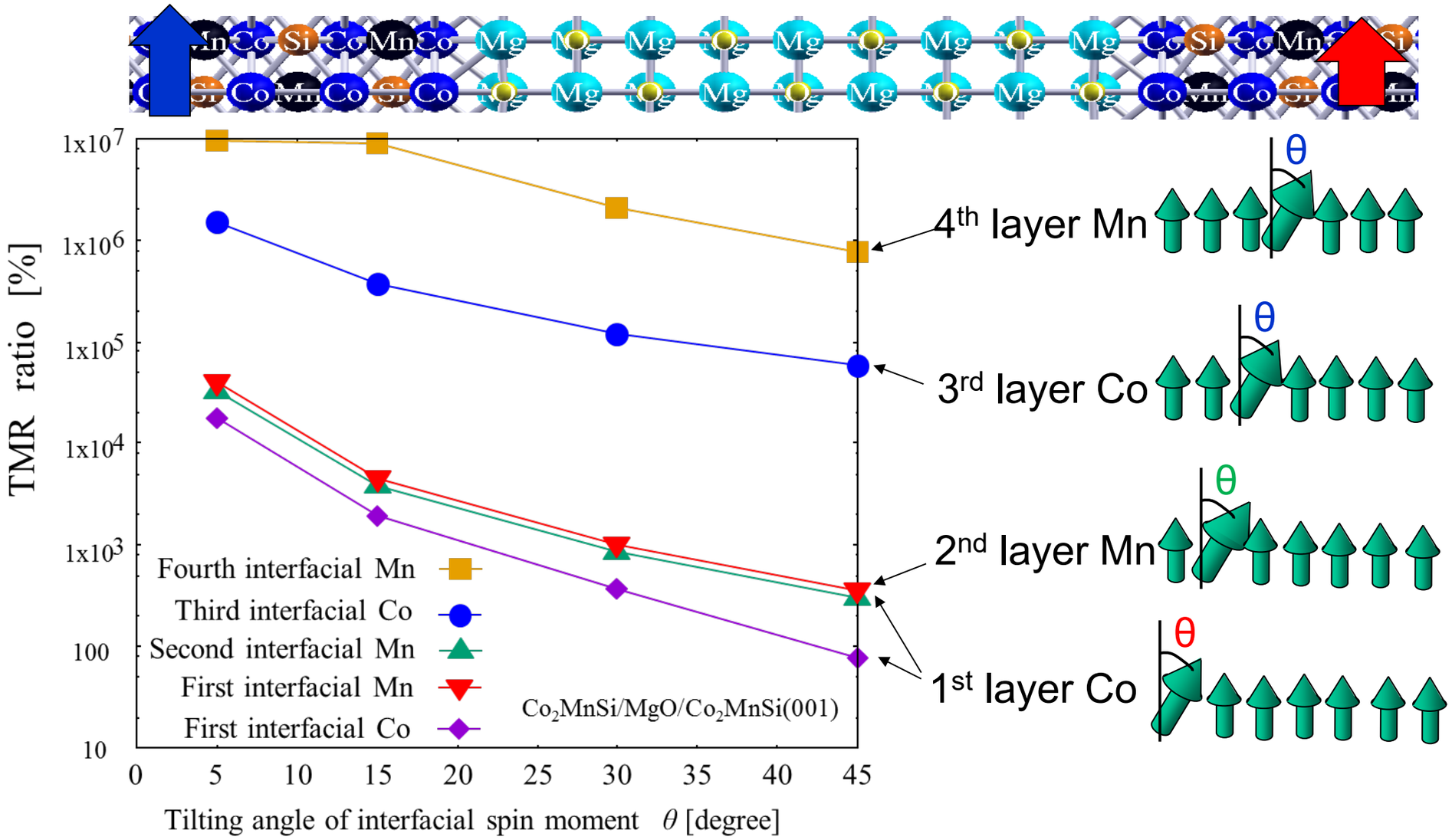

Noncollinear magnetic structures of the first and the second interfacial layer strongly reduce TMR.

Noncollinear magnetic structure of the third and forth interfacial layer show relatively small reduction of TMR.

Exchange stiffness constant at CMS/MgO(001)

Increase of band energy of Non-collinear Spin ⇒ Strength of exchange coupling

$E(\theta)=A(1-\cos\theta)$ $A \propto JM^2$

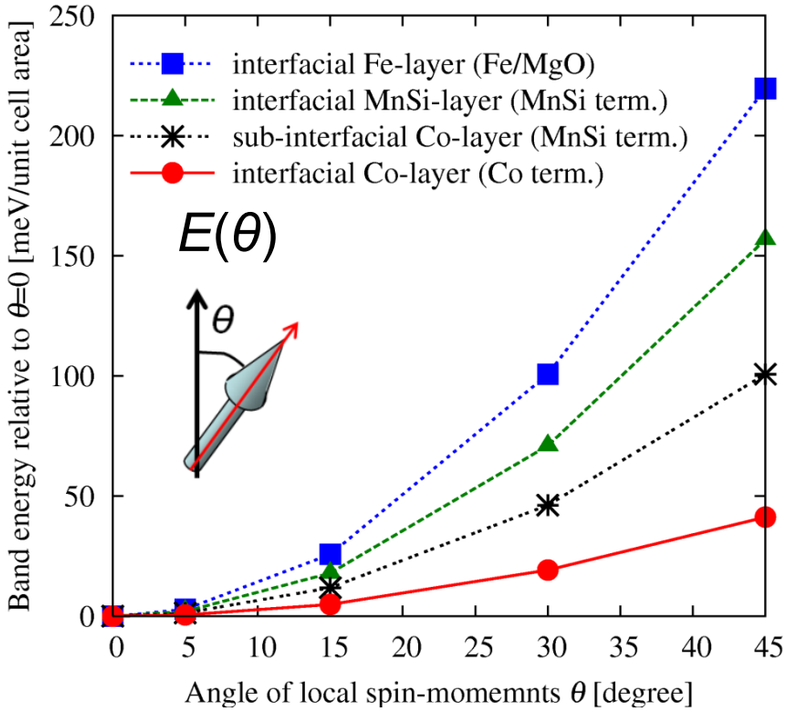

A. Sakuma, *et al.*, JAP **105**, 07C910 (2009).

Off-diagonal part of local potential

$$V_{\alpha\beta(\alpha\neq\beta)}(\mathrm{r}) = \left(\frac{\delta E_{XC}}{\delta n_{\uparrow}} - \frac{\delta E_{XC}}{\delta n_{\downarrow}}\right)\sin\theta$$

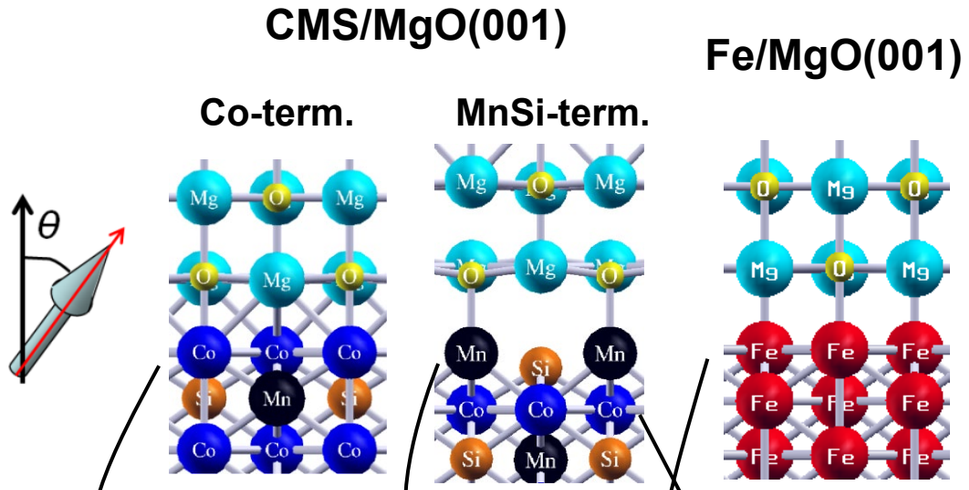

Exchange stiffness of interfacial atoms

A [meV/u.c.a.]	Co^1	Mn^1	Fe^1	Co^2
Bulk (CMS or Fe)	414	529	600	414
MgO interface	145	565	753	347
ΔA [meV/u.c.a.]	−269	+34	+153	−67

Interfacial local spin-moment

M [μ_B]	Co^1	Mn^1	Fe^1
Bulk (CMS or Fe)	0.93	3.31	2.35
MgO interface	0.54	4.06	2.98
ΔM [μ_B]	−0.39	+0.75	+0.63

TMR ratio at finite temperature

Boltzmann average of tunneling conductance

$$t^{(\mathrm{para,anti})}(T) = \frac{\int t_{(\mathrm{para,anti})}(\theta)\exp[-2E(\theta)/k_BT]\sin\theta\, d\theta}{\int \exp[-2E(\theta)/k_BT]\sin\theta\, d\theta}$$

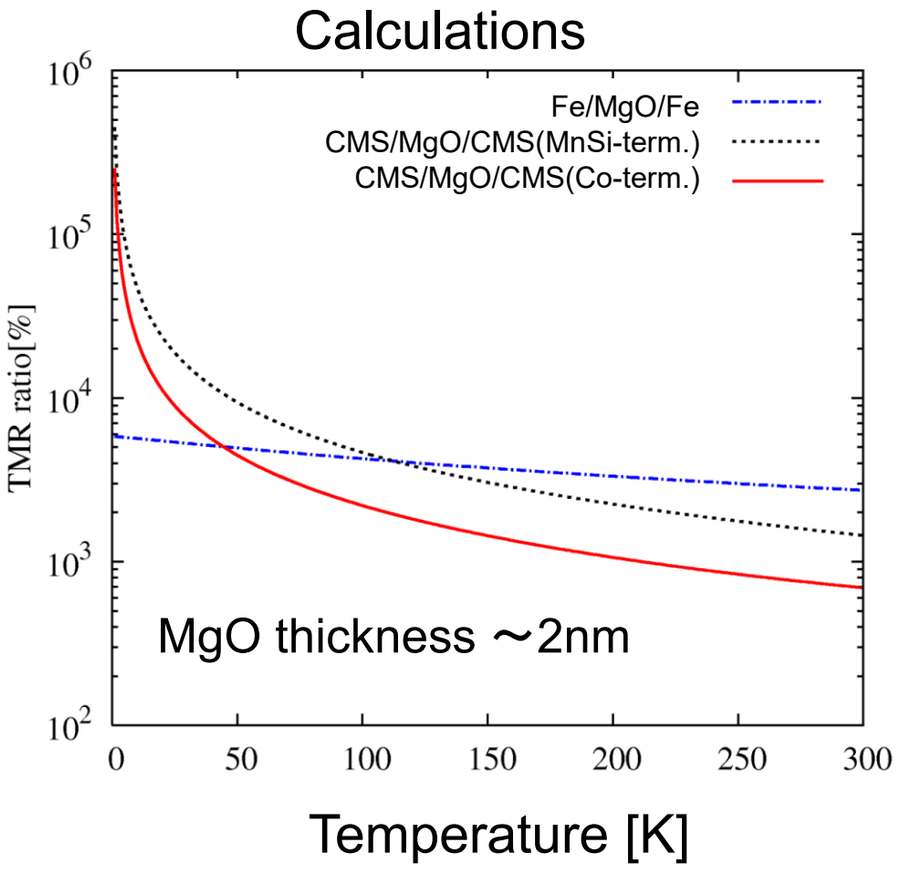

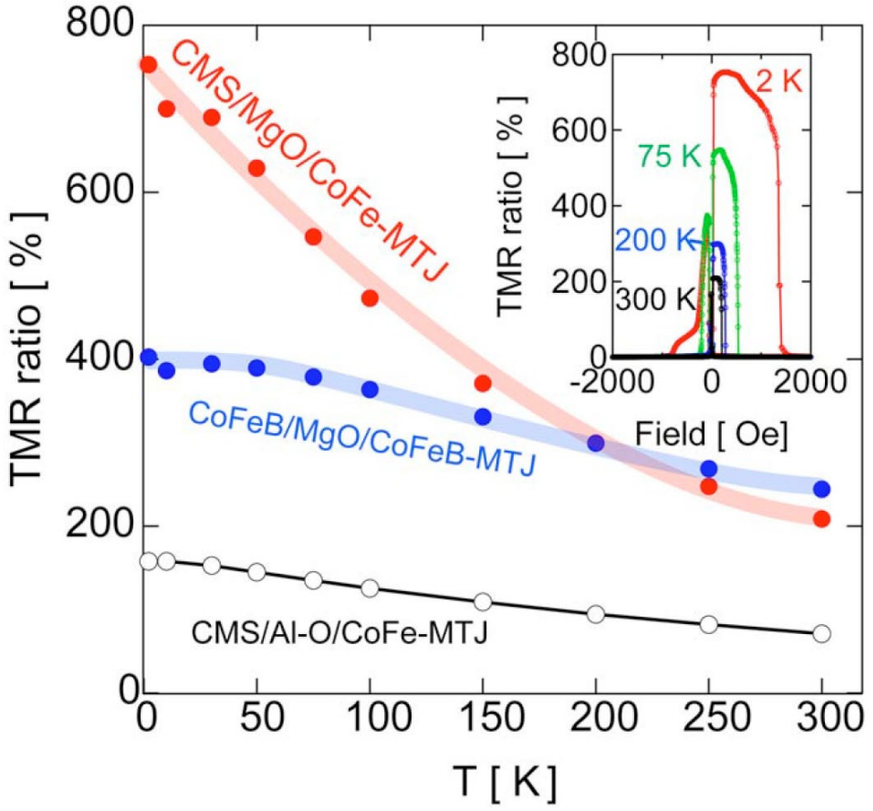

Reduction TMR ratio at RT in CMS/MgO/CMS MTJ can be attributed to a spin-flip scattering at interfacial region caused by thermal fluctuation.

Exchange coupling for other Heusler alloys

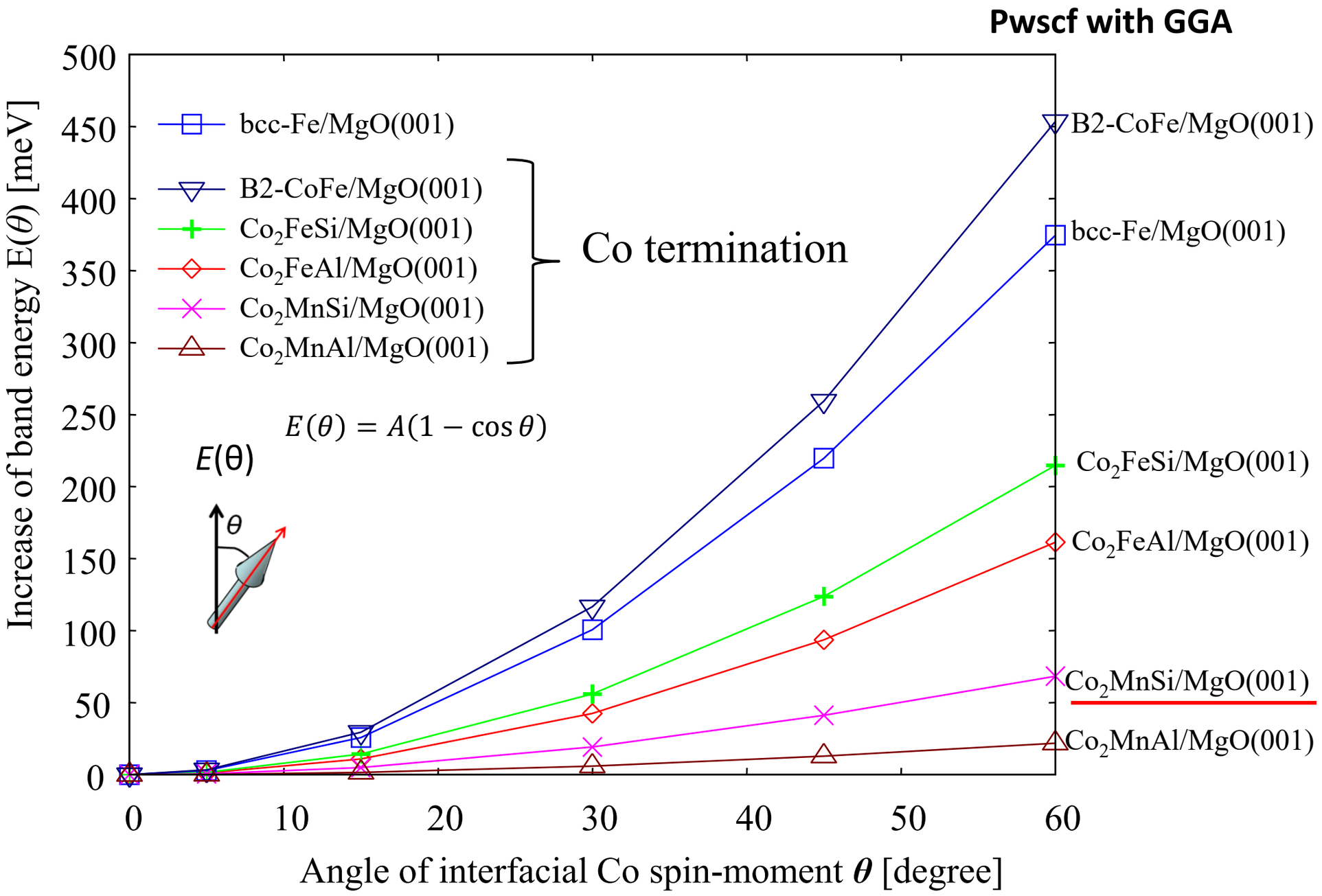

Exchange stiffness constant at Co termination

Inter-atomic layer exchange stiffness constant A [meV/cell area]

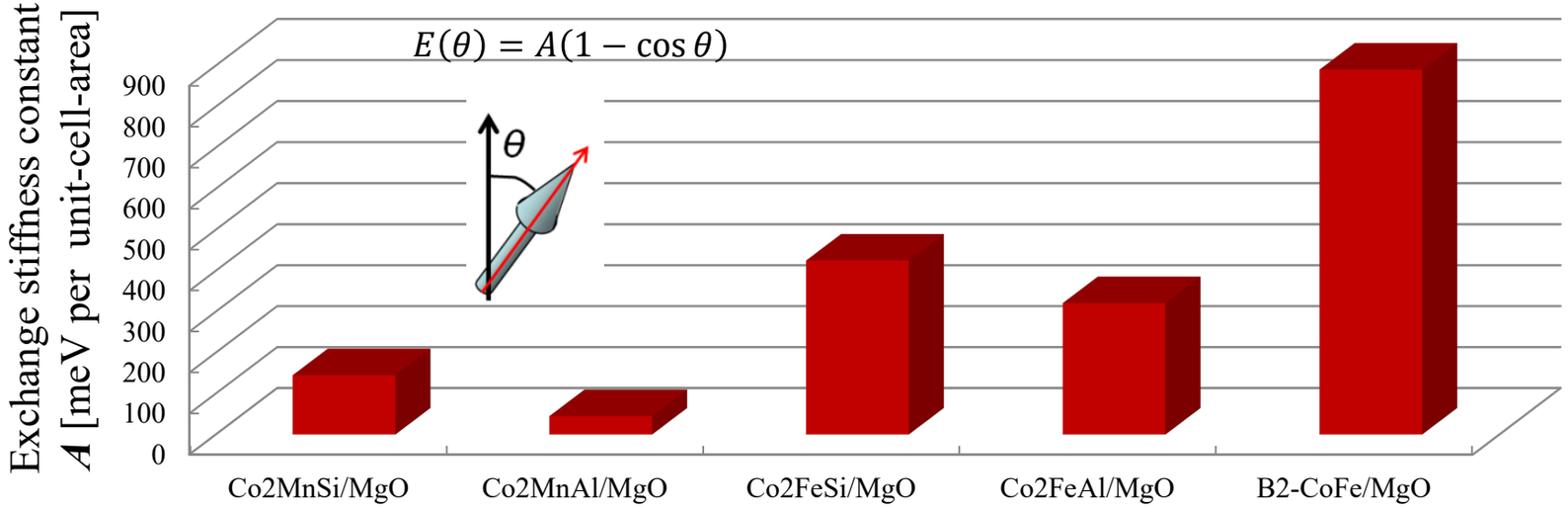

Interfacial Co spin-moment at Co termination [μ_B] $A \propto JM^2$

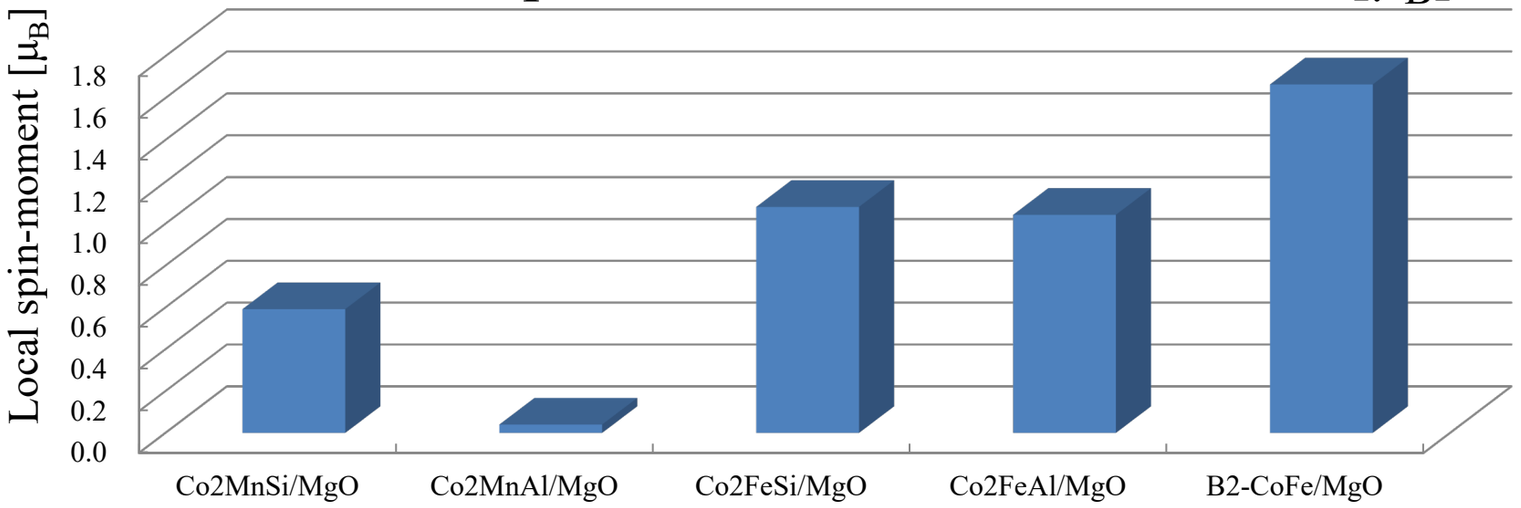

Enhancement of interfacial Co spin-moment is effective to obtain large exchange coupling.

Comparison with Experimental results on TMR at LT and RT

$Co_2MnSi/MgO(001)$

S. Tsunegi, *et al*., APL 93 (2008) 112506.

$$\frac{\text{TMR(RT)}}{\text{TMR(2K)}} = \frac{217\%}{753\%} = 0.29$$

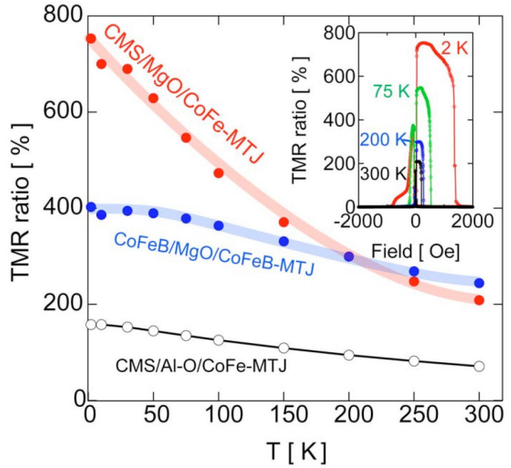

T. Ishikawa, *et al*., APL 94 (2009) 092503.

$$\frac{\text{TMR(RT)}}{\text{TMR(5K)}} = \frac{180\%}{700\%} = 0.26$$

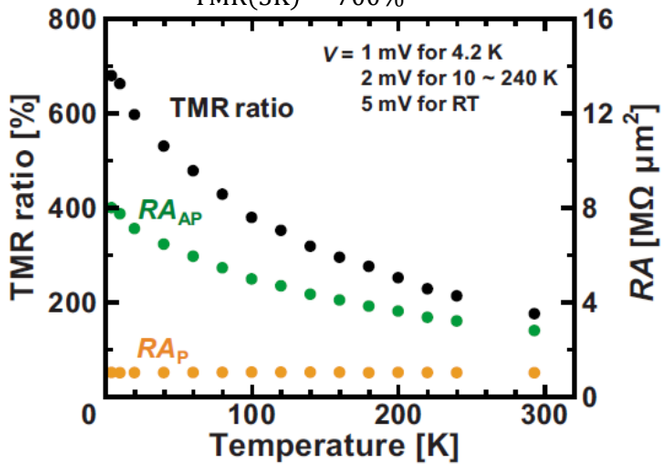

$Co_2Fe(Al,Si)/MgO(001)$

W. Wang, *et al*., APL 95 (2009) 182502.

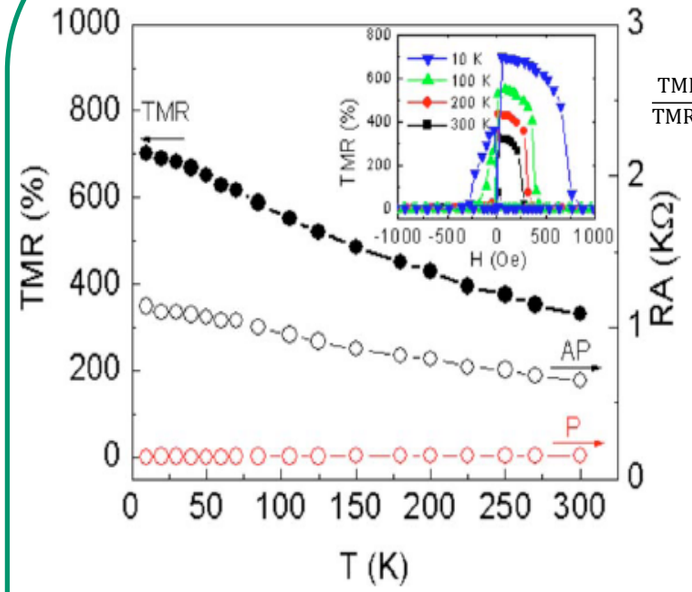

$$\frac{\text{TMR(RT)}}{\text{TMR(10K)}} = \frac{330\%}{700\%} = 0.47$$

N. Tezuka, *et al*., APL 94 (2009) 162504.

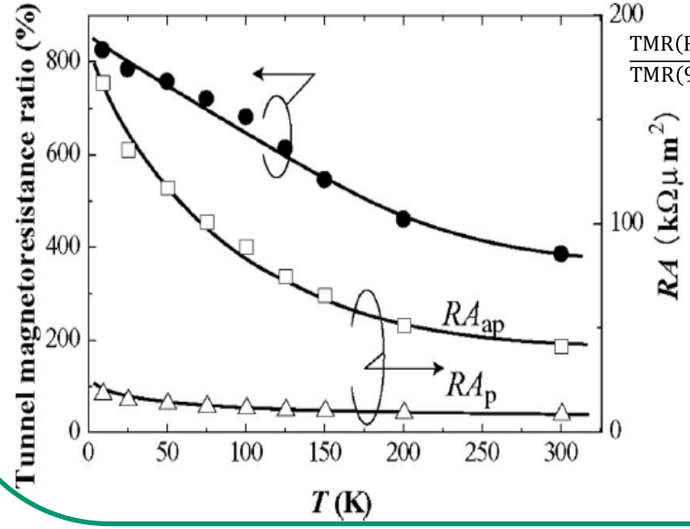

$$\frac{\text{TMR(RT)}}{\text{TMR(9K)}} = \frac{386\%}{832\%} = 0.46$$

New development on TMR

$$\text{TMR比} = 100 \times \frac{R^{\mathrm{AP}} - R^{\mathrm{P}}}{R^{\mathrm{P}}}$$

The highest TMR at 300K was 604% by Tohoku Univ. from 2008 to 2022.

TMR ratio at 300K

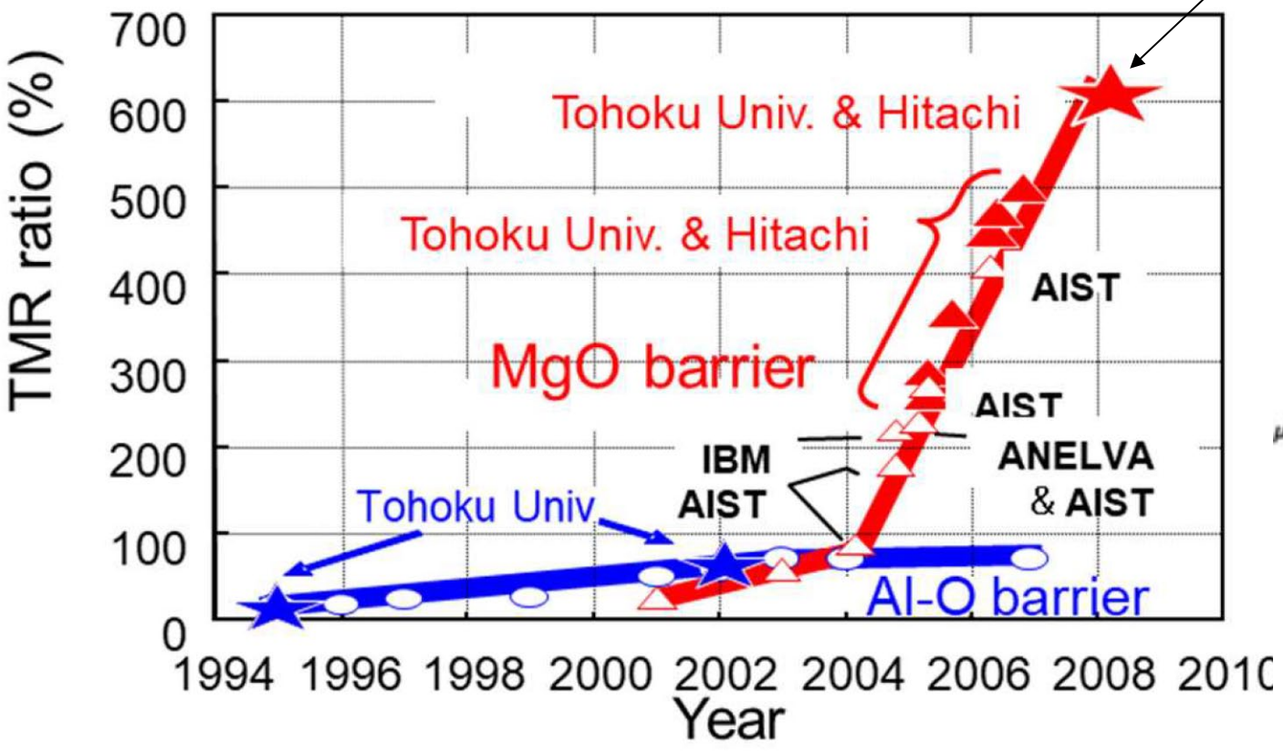

Word record !
by NIMS in 2023

631%

NIMS spintronics group
Appl. Phys. Lett. 122, 112404 (2023)

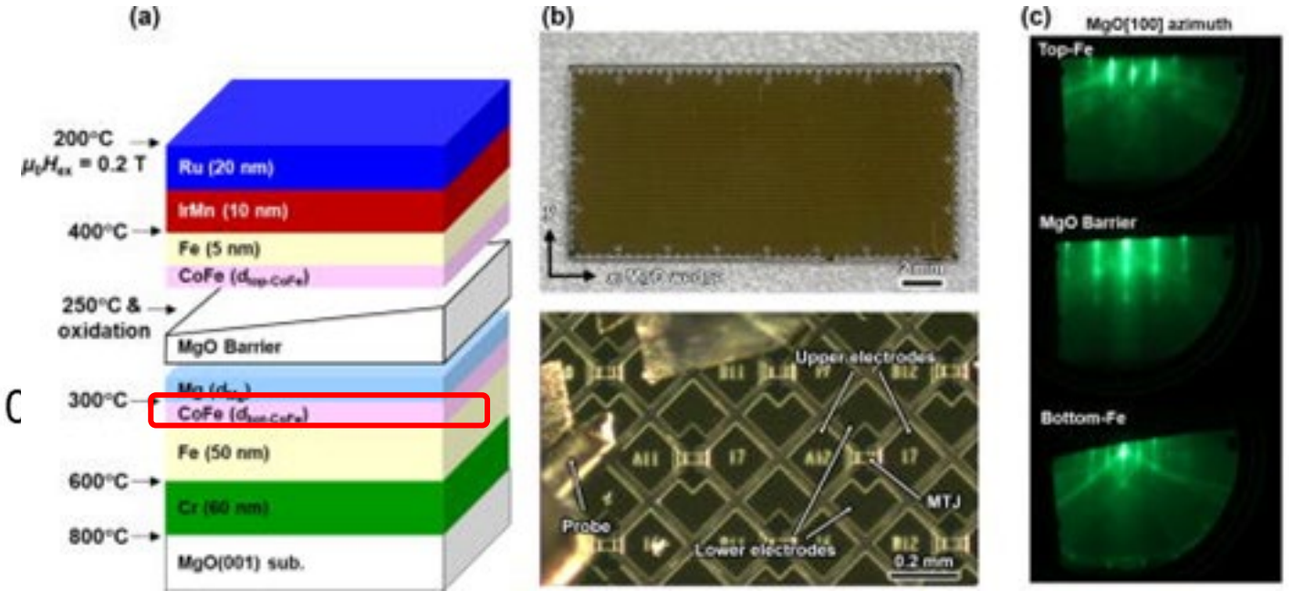

令和３年度　安全保障技術研究推進制度　成果報告書より

Recent progress

More sophisticated treatment of spin-flip scattering at finite temperature in MTJs

K. Masuda, T. Tadano, Y. Miura,
PRB **104**, L180403 (2021).

Spin-flip Hamiltonian

$$H_{sd} = -2J_{sd} \sum_i \boldsymbol{s}_i \cdot \boldsymbol{S}_i$$

J_{sd}: Intra-atomic exchange coupling between conductive s electrons and localized d electrons

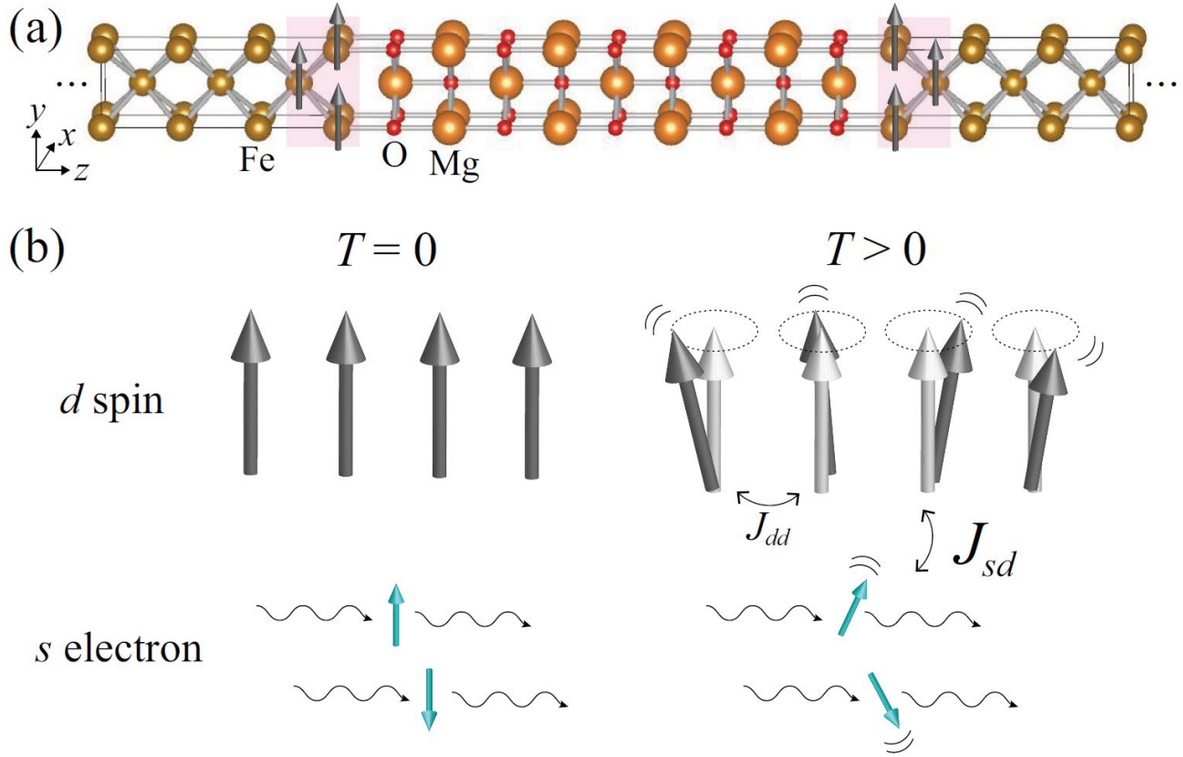

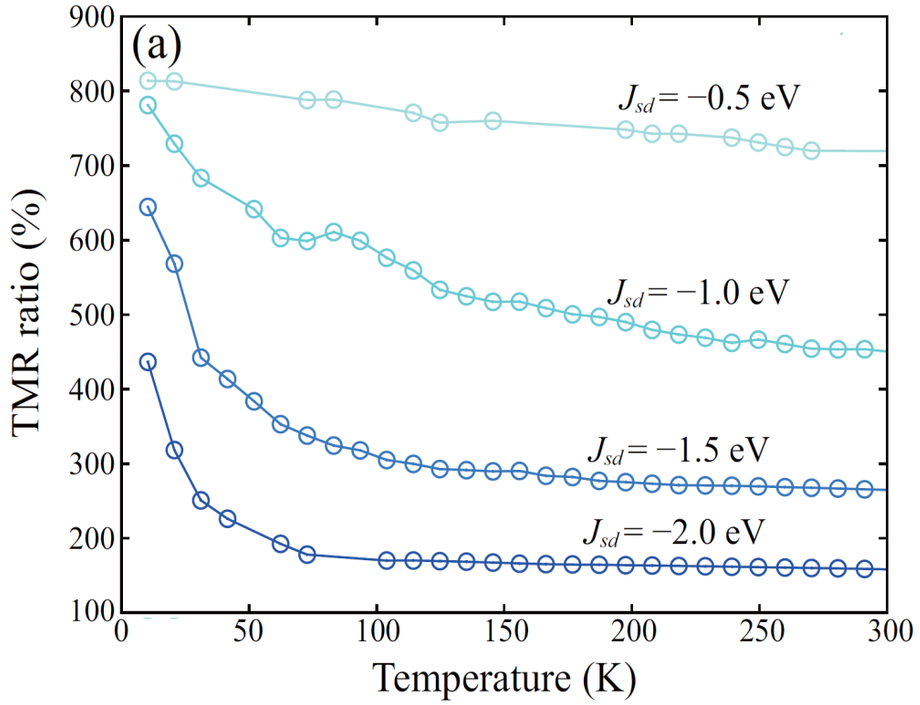

Summary of the first topic

◇ Spin-flip scattering at 1ML of interfacial non-collinear spin strongly reduces the TMR.

◇ Interfacial Co-layer is easy to fluctuate at RT due to the small exchange stiffness at CMS/MgO(001).

◇ The reduction of the TMR ratio at RT can be attributed to spin-flip scattering at interfacial region caused by thermal fluctuation of interfacial Co-layers.

To raise the TMR ratio at RT, we have to insert CoFe-layer to enhance the interfacial exchange stiffness of CMS/MgO.

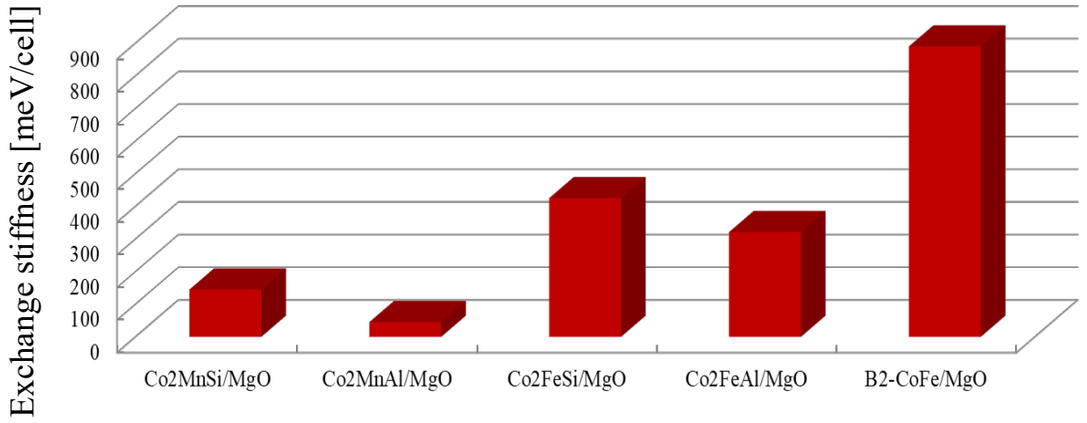

Topics

1. Introduction on spintronics

2. Spin-dependent transport in magnetic tunnel junctions with half-metallic Heusler alloys

Y. Miura, *et al*., PRB **83,** 214411 (2011).

K. Masuda, T. Tadano, Y. Miura, PRB **104**, L180403 (2021).

3. First-Principles Study on magnetic damping of Fe(001) interface

R. Mandal, et al., Phys. Rev. Applied **14**, 064027 (2020).

What is magnetic damping?

Dynamics in local spin moment

External magnetic field ***H***

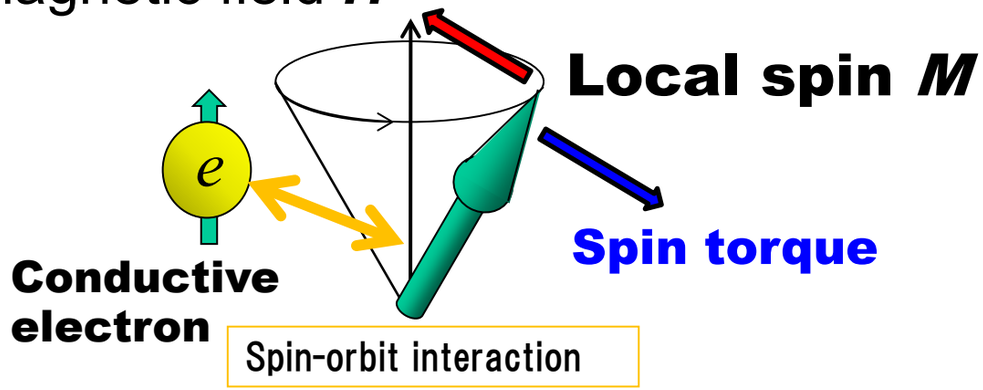

Critical current density in STT switching

$$J_{c0} \propto \alpha M_S [H_{\text{anti}} \pm 4\pi M_S]\ t/P$$

Equation of motion of magnetization
Landau-Lifshitz-Gilbert (LLG)

$$\frac{d\vec{M}}{dt} = -\gamma\left(\vec{M}\times\vec{H}\right) - \frac{\lambda}{M_s^2}\left(\vec{M}\times\left(\vec{M}\times\vec{H}\right)\right)$$

Spin torque **Damping torque**

$$\begin{cases} \lambda = \alpha\gamma M_s \\ \gamma = \mu_0 g \mu_B / \hbar \end{cases}$$

α : magnetic damping

M_s : Saturation magnetization

γ : Gyromagnetic constant

Right circular dichroism of magnetic field

$$\vec{H} = H^+\left(\vec{e}_x + i\vec{e}_y\right)\exp\left(-i\omega t\right) + H_{eff}\vec{e}_z$$

Precession motion of Local spin moment

$$\vec{M} = M^+\left(\vec{e}_x + i\vec{e}_y\right)\exp\left(-i\omega t\right) + M_s\vec{e}_z$$

$$\Rightarrow\quad M^+ = \chi^+(\omega)H^+$$

Magnetic Susceptibility

$$\chi^+(\omega) = -\frac{\gamma M_s}{\omega - \gamma H_{eff} + i\alpha\omega}$$

Kambersky Torque correlation model

V. Kambersky, Czechoslovak Journal of Physics B **26**, 1366 (1976).

Brownian motion of particle

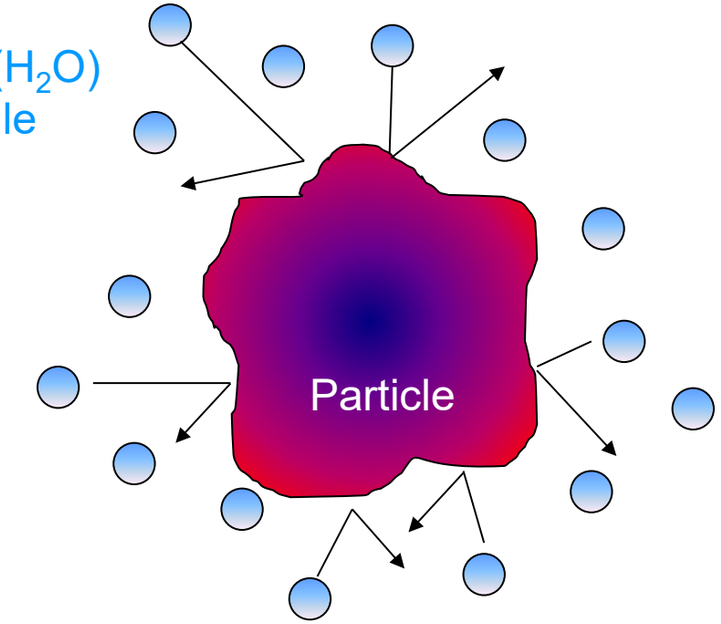

Newton equation of particle in isolate system

Separation of fast motion (random term) and slow motion (friction term) by projection operator method

（Mori-formalism）

Generalized Langevin equation（GLE)

Magnetic damping in precession motion of local spin moment

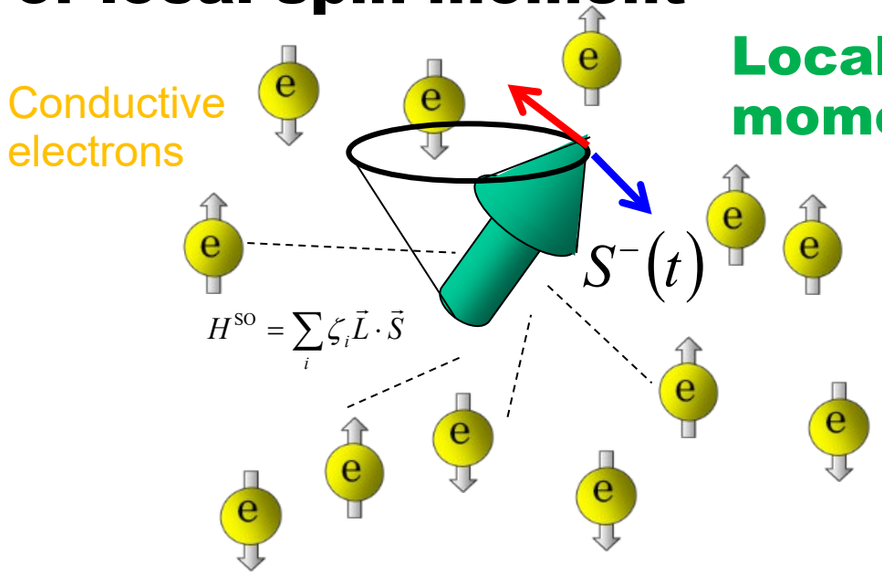

Heisenberg equation of magnetization in isolate system

Separation of fast motion(random term: spin-torque) and slow motion (friction term: damping) by projection operator method

（Mori-formalism）

Generalized Langevin equation（GLE)

Microscopic theory of magnetic damping

Separation between fast motion and slow motion (Mori formalism)

V. Kambersky, Czechoslovak Journal of Physics B **26**, 1366 (1976).

$$\frac{dS^-(t)}{dt} = -i\Omega S^-(t) - \int_0^t (\hbar M)^{-1} \left\langle \left[\phi^-(t'), \phi^+\right] \right\rangle_0 S^-(t-t')dt' - i\phi^-(t)$$

Spin torque operator

$$\phi^-(t) = \left[S^-(t), H^{SO}\right]$$

Precession motion

Friction（damping）term (slow motion)

Random（spin-torque）term (fast motion)

Projection to S^+

$$\frac{d\left\langle \left[S^-(t), S^+\right] \right\rangle_0}{dt} = -i\Omega \left\langle \left[S^-(t), S^+\right] \right\rangle_0 - \int_0^t (\hbar M)^{-1} \left\langle \left[\phi^-(t'), \phi^+\right] \right\rangle_0 \left\langle \left[S^-(t), S^+\right] \right\rangle_0 dt'$$

Laplace transform

$$\chi_0^+(\omega + i\varepsilon) = \frac{\hbar M}{\omega + i\varepsilon - \Omega - (\hbar M)^{-1} f(\omega + i\varepsilon)}$$

Fourier transform of correlation function of spin-torque (two-point Green's function)

$$F(\omega + i\varepsilon) = -i\int_{-\infty}^{\infty} \left\langle \left[\phi^-(t), \phi^+\right] \right\rangle_0 \theta(t) e^{i(\omega + i\varepsilon)t} dt$$

代入

Random phase approximation (RPA)

Magnetic susceptibility

$$\chi^+(\omega) = -\frac{\mu_0 (g\mu_B)^2}{\hbar V} \frac{\hbar M}{\omega + i\varepsilon - (\Omega - \Delta) - (\hbar M)^{-1} F(\omega + i\varepsilon)}$$

Kambersky torque correlation model

Microscopic formulation of magnetic susceptibility

$$\chi^{+}(\omega)=-\frac{\mu_0(g\mu_B)^2}{\hbar V}\frac{\hbar M}{\omega+i\varepsilon-(\Omega-\Delta)-(\hbar M)^{-1}F(\omega+i\varepsilon)}$$

Macroscopic formulation of magnetic susceptibility

$$\chi^{+}(\omega)=-\frac{\gamma M_s}{\omega-\gamma H_{eff}+i\alpha\omega}$$

Magnetic damping

$$\lambda=-\lim_{\omega\to 0}\frac{\gamma^2}{\hbar\mu_0 V}\mathrm{Im}\left[\frac{1}{\omega}F(\omega+i\varepsilon)\right]$$

$$F(\omega+i\varepsilon)=-i\int_{-\infty}^{\infty}\left\langle\left[\phi^{-}(t),\phi^{+}\right]\right\rangle_0\theta(t)e^{i(\omega+i\varepsilon)t}dt$$

（Calculation of Green's function）

$$\lambda=\frac{g^2\mu_0\mu_B^2}{\pi\hbar V}\sum_{\vec{k}}\sum_{nm}\left|\Gamma_{nm}^{-}(\vec{k})\right|^2\frac{\delta}{\left(E_F-E_{n\vec{k}}\right)^2+\delta^2}\frac{\delta}{\left(E_F-E_{n\vec{k}}\right)^2+\delta^2}$$

Matrix elements of torque operator

$$\Gamma_{nm}^{-}(\vec{k})=\left\langle n,\vec{k}\left|\left[S^{-},H^{\mathrm{SO}}\right]\right|m,\vec{k}\right\rangle$$

Spin torque operator

$$\left[S^{-},H^{\mathrm{SO}}\right]=\zeta\left(S^{-}L^{z}-S^{z}L^{-}\right)$$

Spin-flip term

Spin-conserving term

$$\lambda\approx\zeta\frac{\mu_B^2}{\pi\hbar}\int D(E_F)\frac{\delta}{\varepsilon^2+\delta^2}d\varepsilon$$

Magnetic damping depends on DOS at E_F and spin-orbit constant ζ.

First-principles calculation of magnetic damping

$$\lambda = \frac{g^2 \mu_0 \mu_B^2}{\pi \hbar V} \sum_{\vec{k}} \sum_{nm} \left| \Gamma_{nm}^{-}\left(\vec{k}\right) \right|^2 \frac{\delta}{\left(E_F - E_{n\vec{k}}\right)^2 + \delta^2} \frac{\delta}{\left(E_F - E_{n\vec{k}}\right)^2 + \delta^2} \qquad \alpha = \frac{\gamma M_s}{\lambda} \qquad \gamma = \mu_0 g \mu_B / \hbar$$

Energy eigenvalue at each k and band n.

$$\Gamma_{nm}^{-}\left(\vec{k}\right) = \left\langle n, \vec{k} \left| \zeta \left(S^- L^z - S^z L^- \right) \right| m, \vec{k} \right\rangle$$

Calculation of matrix elements of spin-torque operator using wavefunctions in DFT calculations

Bulk-Fe

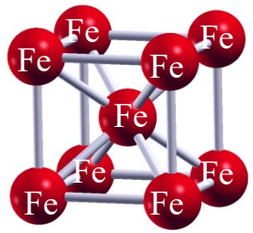

μ_s=2.207μ_B

μ_l=0.049μ_B

α=0.00105

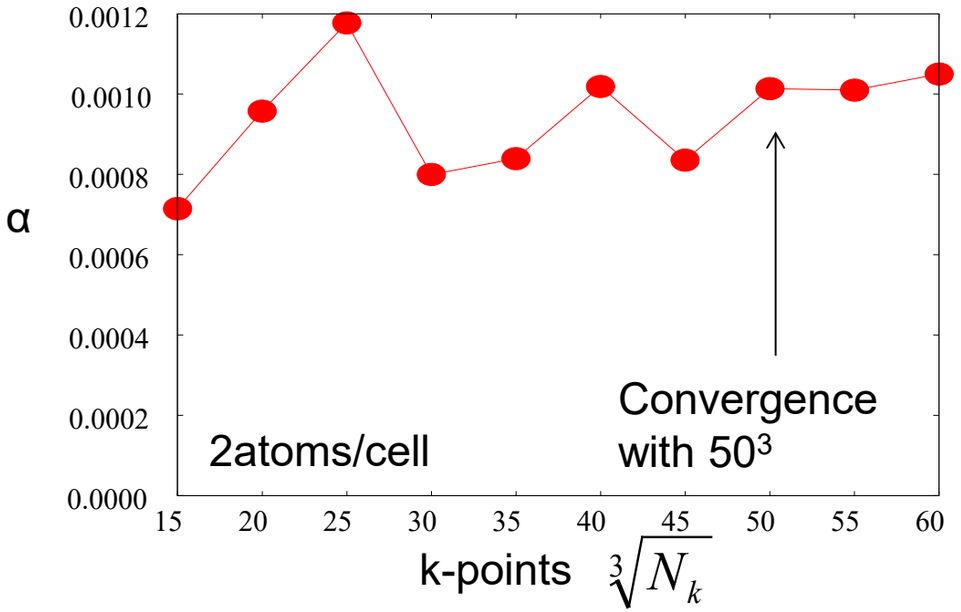

⇒For surface and interface, 50x50 k-points are necessary.

Magnetic damping of ferromagnetic metals

K. Gilmore, PRL **99,** 027204 (2007)

Experiments

	α_{calc}	λ_{calc}	λ_{meas}	$\lambda_{calc}/\lambda_{meas}$	$(\lambda/\tau)_{intra}$	$(\lambda/\tau)_{BFS}$
bcc Fe ⟨001⟩	0.0013	0.54	0.88	0.61	1.01	0.968
bcc Fe ⟨111⟩	0.0013	0.54	⋯	⋯	1.35	1.29
hcp Co ⟨0001⟩	0.0011	0.37	0.9	0.41	0.786	0.704
fcc Ni ⟨111⟩	0.017	2.1	2.9	0.72	6.67	6.66
fcc Ni ⟨001⟩	0.018	2.2	⋯	⋯	8.61	8.42

Intra-band transition
（conductivity term）

Inter-band transition
（resistivity term）

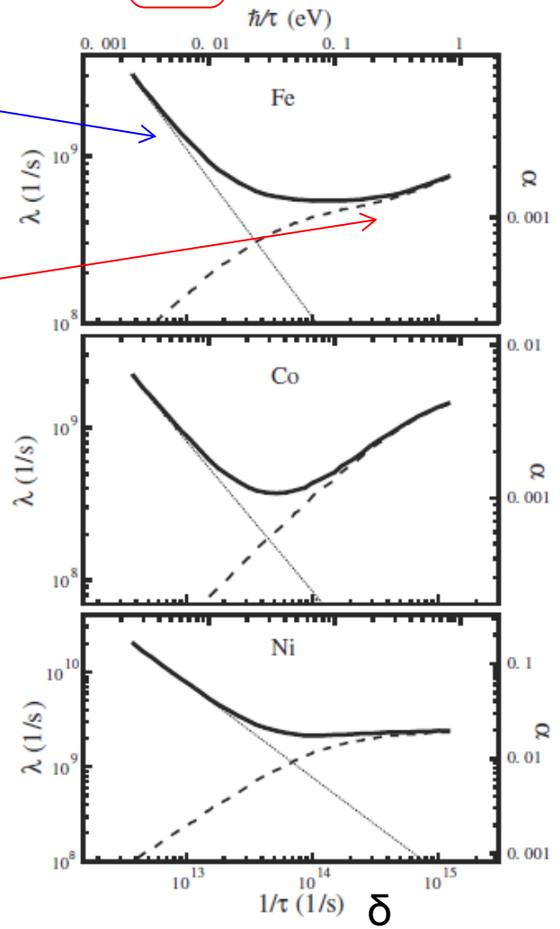

Comparison with Density of states (DOS)

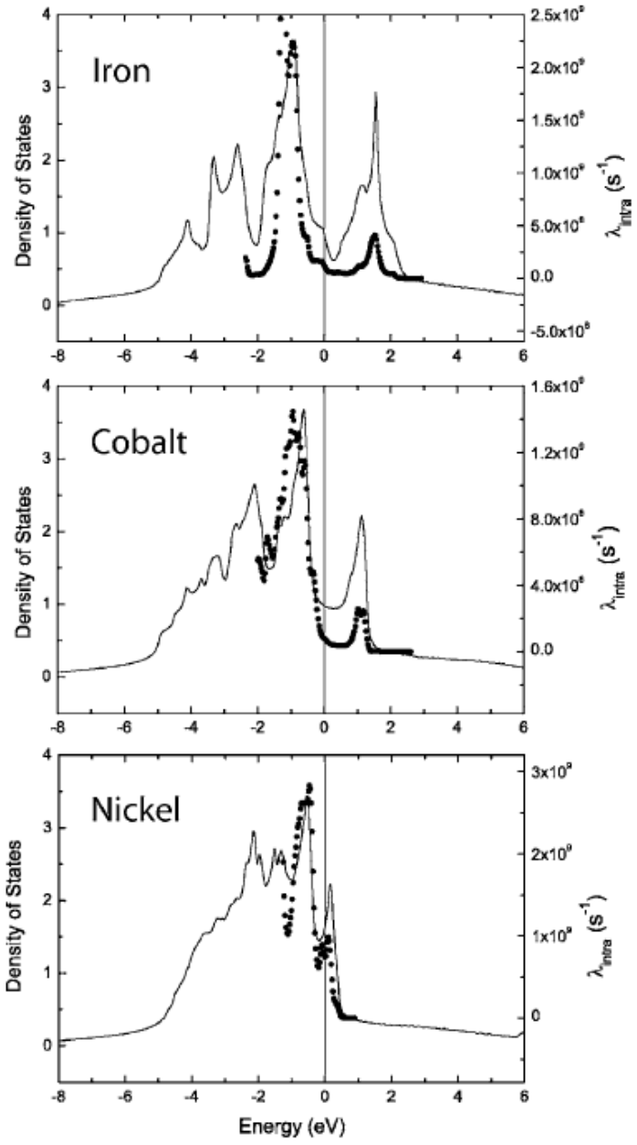

Another application: Voltage controlled magnetic anisotropy (VCMA) switching in MTJ

Applied Physics Express **9**, 013001 (2016)
http://doi.org/**10.7567/APEX.9.013001**

Evaluation of write error rate for voltage-driven dynamic magnetization switching in magnetic tunnel junctions with perpendicular magnetization

Yoichi Shiota*, Takayuki Nozaki, Shingo Tamaru, Kay Yakushiji, Hitoshi Kubota, Akio Fukushima, Shinji Yuasa, and Yoshishige Suzuki

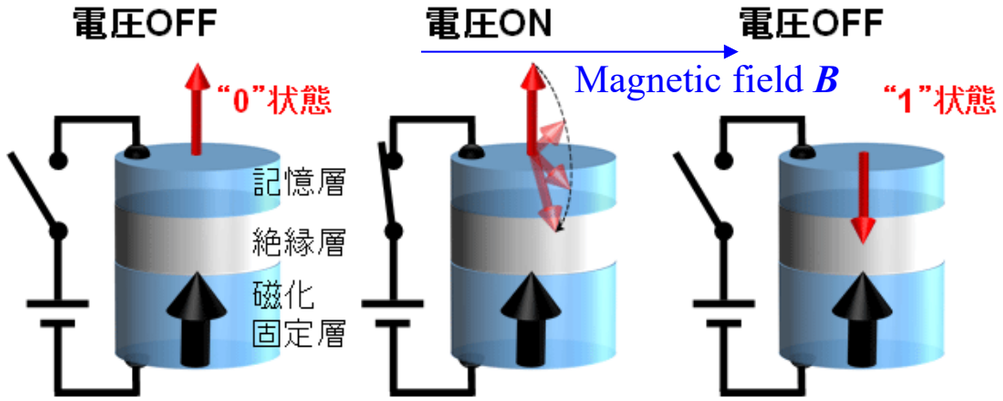

From website of Sahashi's ImPACT project in JST

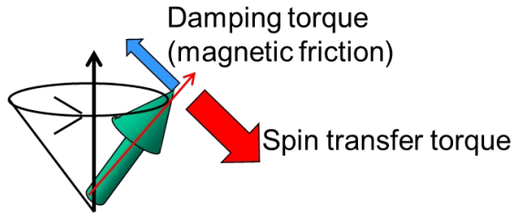

Write Error Rate (WER)

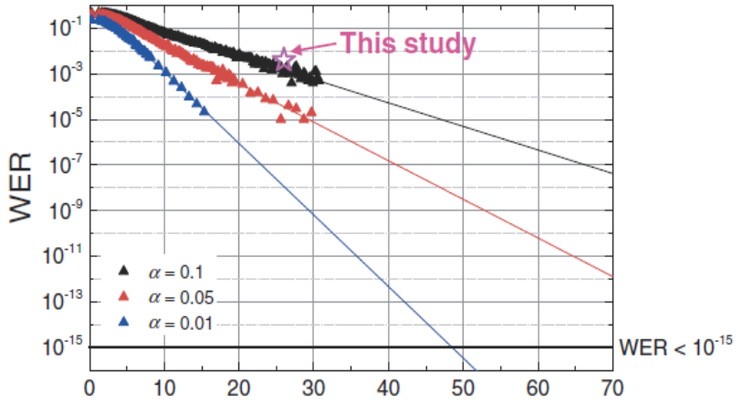

Fig. 4. Calculated WER as a function of Δ for fixed tilted magnetization angle and half precession period τ_{pulse} for various damping constants.

Pulsed bias voltage changes PMA (perpendicular magnetic anisotropy) of interface of FM layer and promote the precession motion of the magnetization under uniform magnetic field.

- By removing the voltage with a proper pulse duration, such as a half precession period, magnetization switching can be achieved.
- Basically, no current flow

Large PMA and Small damping α can reduce the WER

Experiments electric field effects of PMA and magnetic damping

APPLIED PHYSICS LETTERS **105**, 052415 (2014)

Electric-field effects on magnetic anisotropy and damping constant in Ta/CoFeB/MgO investigated by ferromagnetic resonance

A. Okada,[1] S. Kanai,[1] M. Yamanouchi,[1,2] S. Ikeda,[1,2] F. Matsukura,[3,2,a)] and H. Ohno[1,2,3]
[1]*Laboratory for Nanoelectronics and Spintronics, Research Institute of Electrical Communication, Tohoku University, 2-1-1 Katahira, Aoba-ku, Sendai 980-8577, Japan*
[2]*Center for Spintronics Integrated Systems, Tohoku University, 2-1-1 Katahira, Aoba-ku, Sendai 980-8577, Japan*
[3]*WPI-Advanced Institute for Materials Research (WPI-AIMR), Tohoku University, 2-1-1 Katahira, Aoba-ku, Sendai 980-8577, Japan*

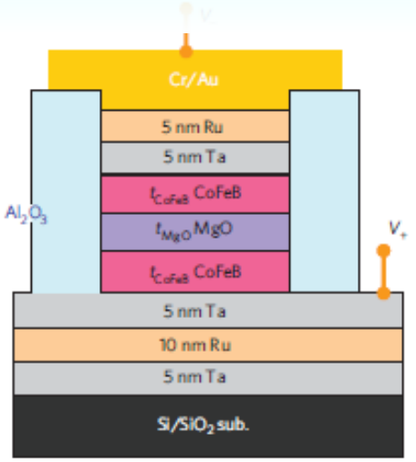

Magnetic anisotropy change by EF

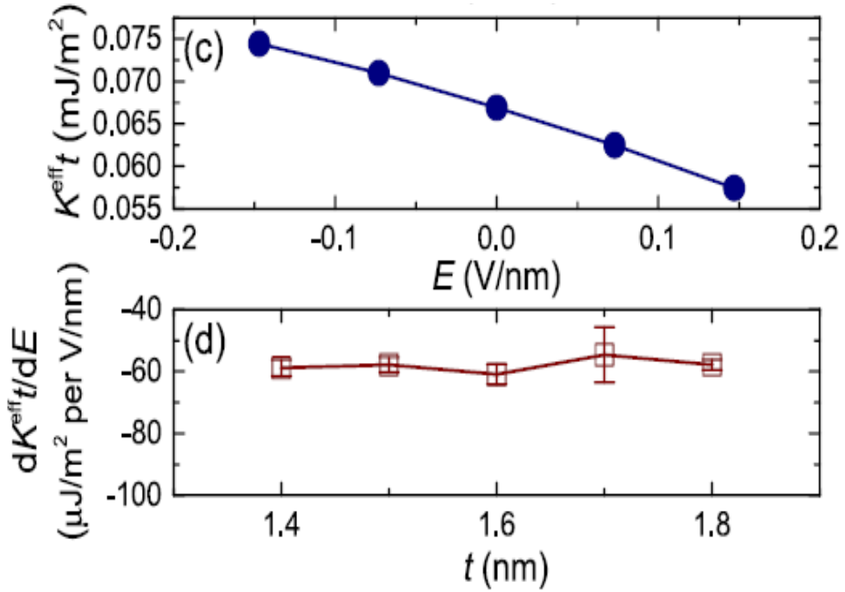

EF dependence is insensitive to thickness of FM layer

Magnetic damping change by EF

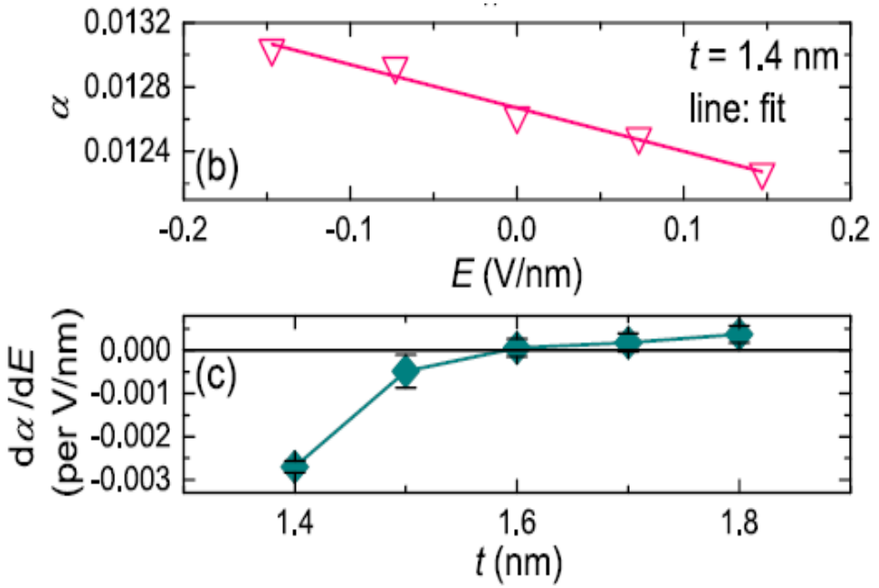

Large thickness dependence of FM layer

-21% of magnetic damping α is changed by 1V/nm EF for t=1.4nm

Potential and charge for model system

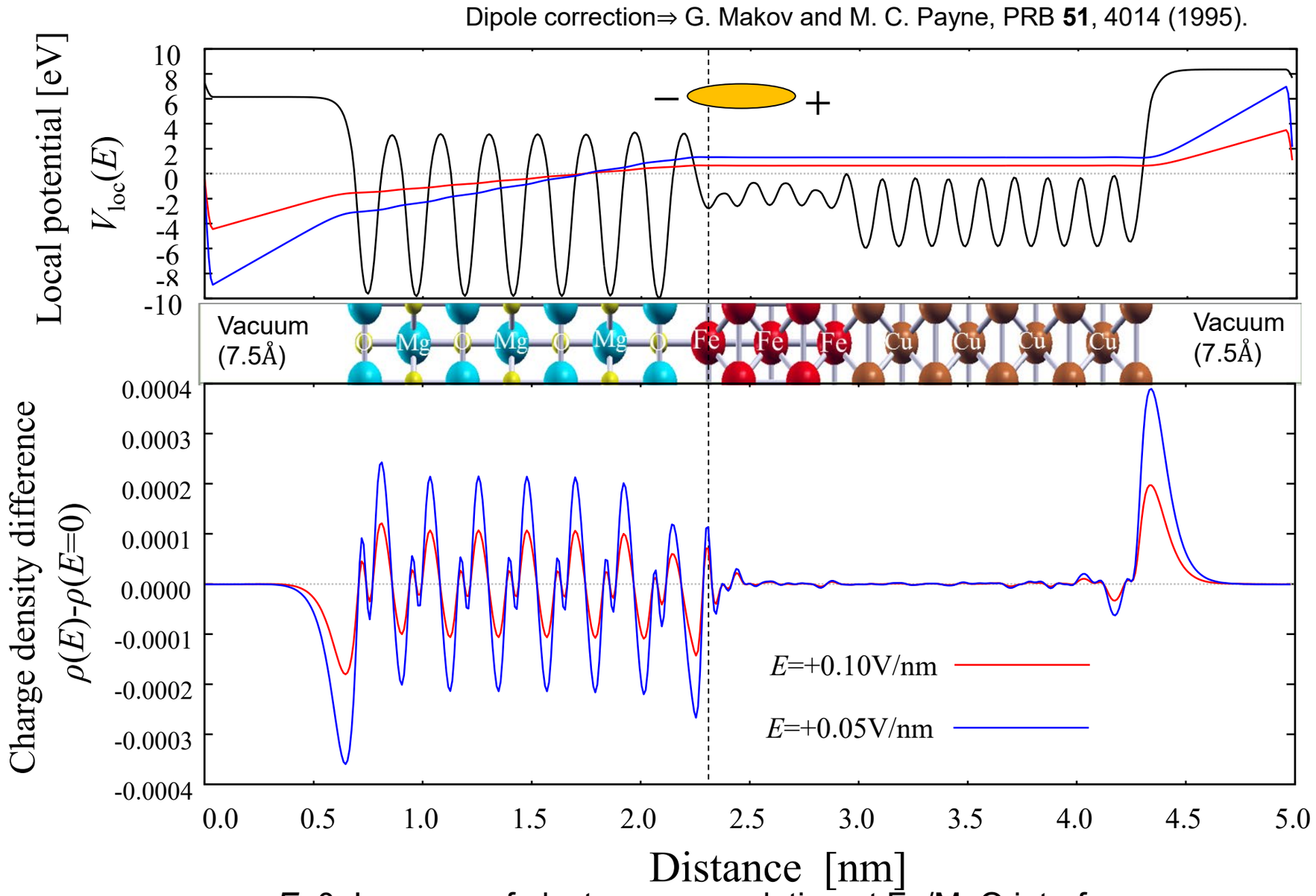

E>0 :Increase of electron accumulation at Fe/MgO interface

E<0 :Decrease of electron accumulation at Fe/MgO interface

Voltage dependence of PMA and damping α of Fe surface and Fe/MgO interface

Fe(001) surface

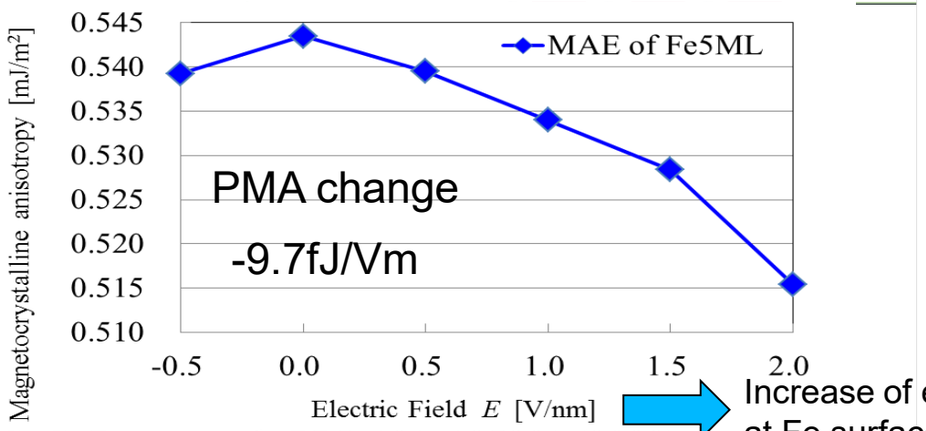

Increase of electron at Fe surface

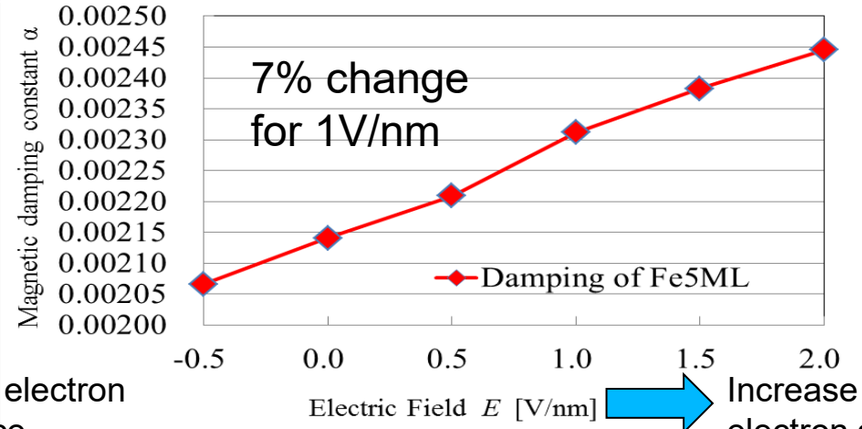

Increase of electron at Fe surface

C. G. Duan, *et al.*, PRL **101**, 137201 (2008).

Fe/MgO(001) interface

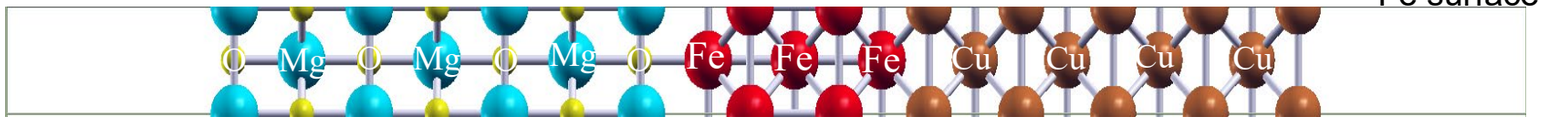

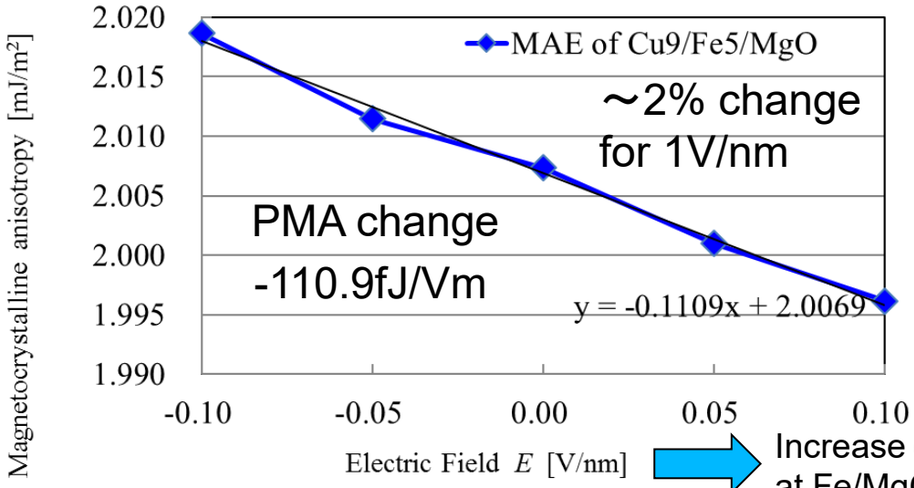

Increase of electron at Fe/MgO interface

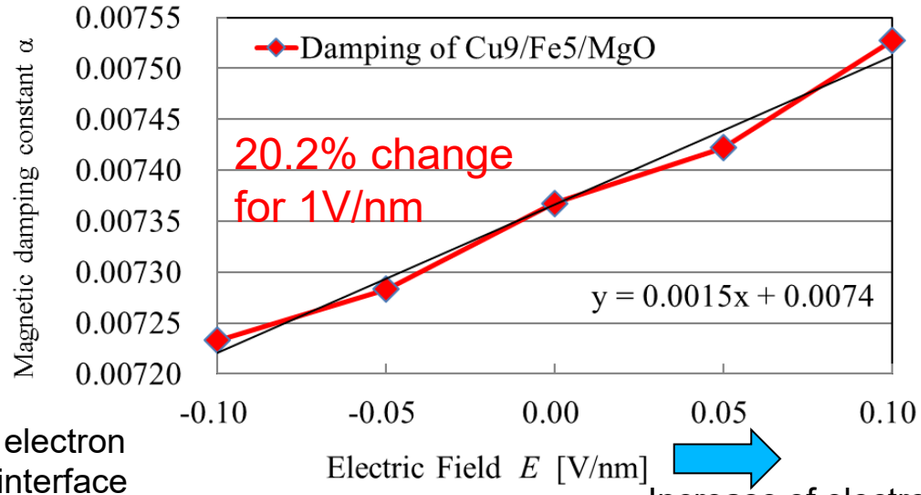

Increase of electron at Fe/MgO interface

Decomposition of magnetic damping α

Torque operator $\Gamma^- = \left[S^-, H^{SO}\right] = \zeta\left(S^z L^- - S^- L^z\right)$

Spin conserving (Orbital deexcitation) term

$\left\langle u^\sigma \left| L^- \right| o^\sigma \right\rangle$

The matrix elements are non-zero for atomic orbitals between different magnetic quantum number, such as d(yz,zx)-d(z^2), d(yz,zx)-d(x^2-y^2), d(yz,zx)-d(xy)

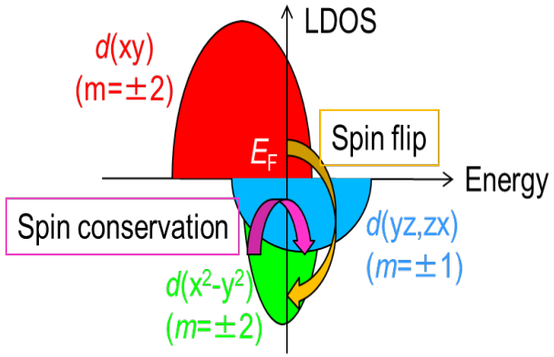

Spin flip (Orbital conservation) term

$\left\langle u^{-\sigma} \left| L_Z \right| o^\sigma \right\rangle$

The matrix elements are non-zero for atomic orbitals between same magnetic quantum number, such as d(yz)-d(zx),d(x^2-y^2)-d(xy)

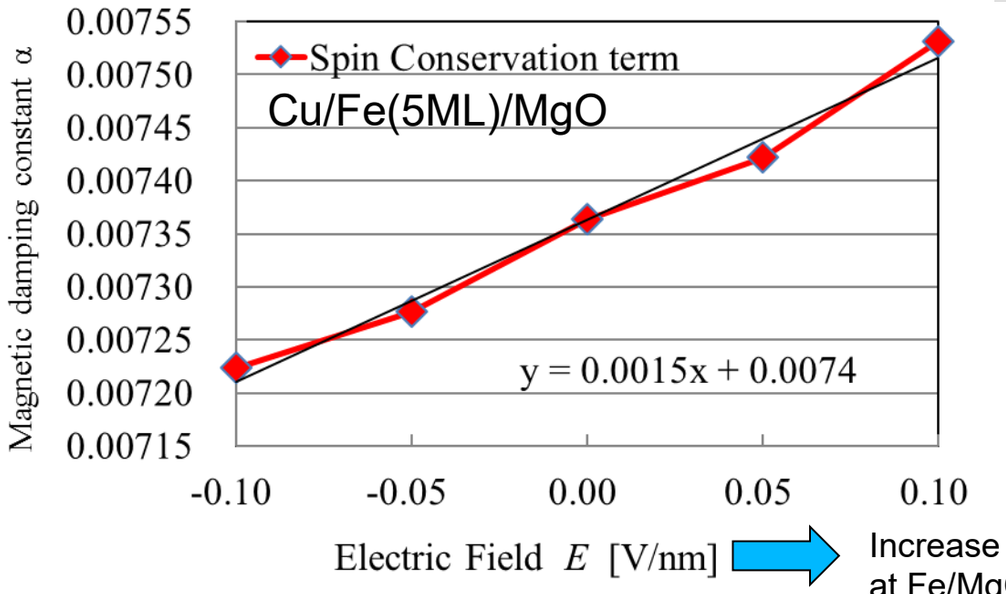

Increase of electron at Fe/MgO interface

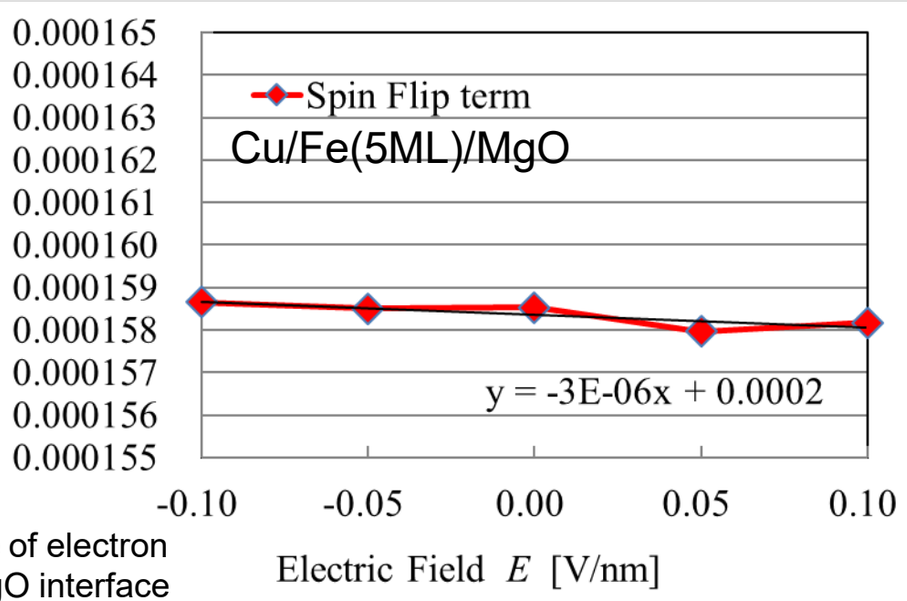

Origin of electric filed dependence

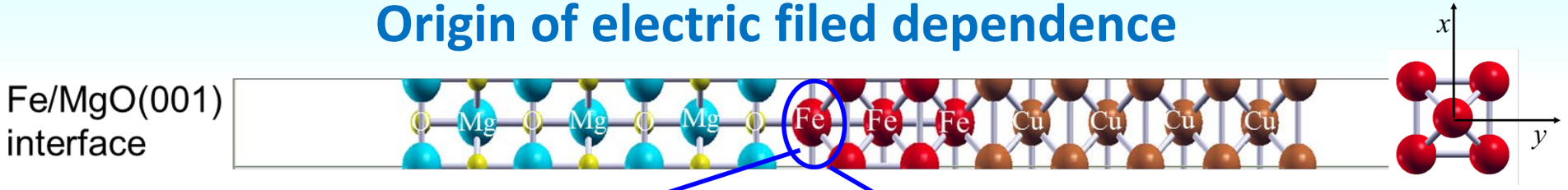

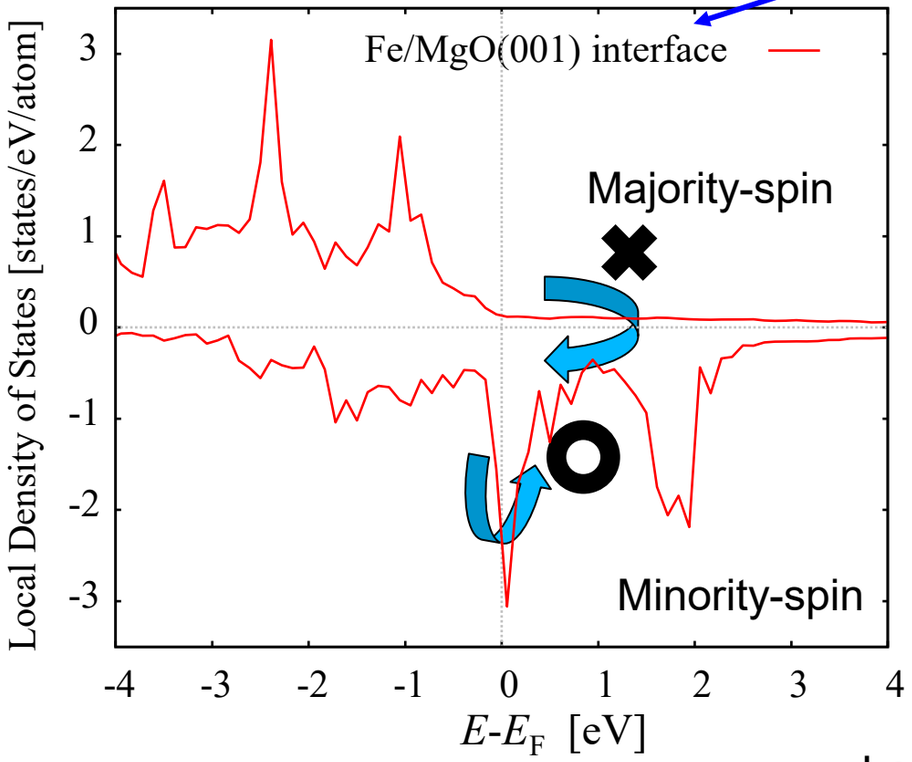

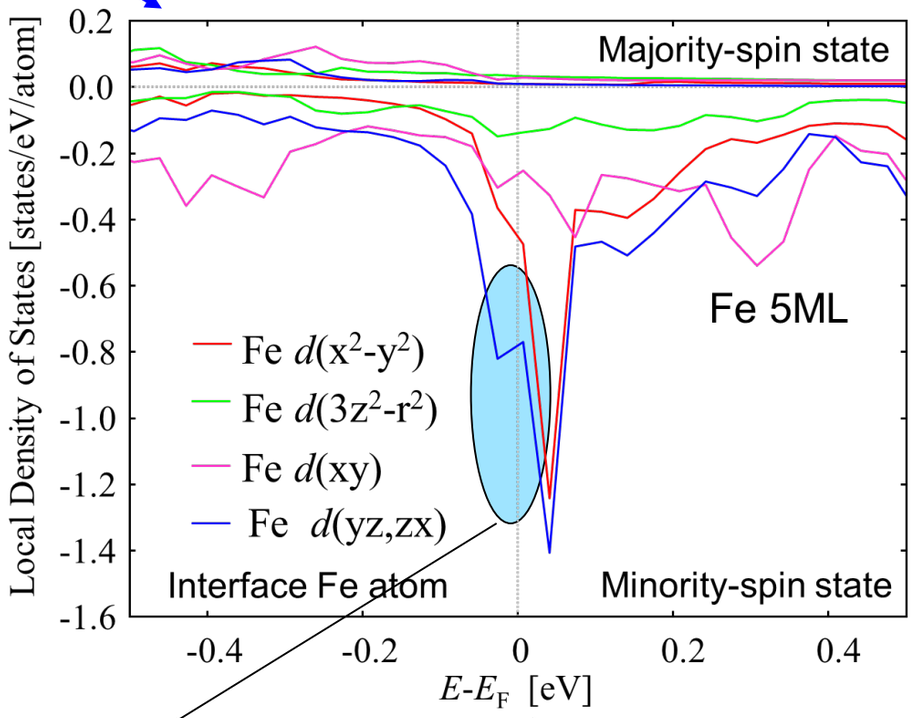

Large matrix element of $\left\langle d\left(x^2-y^2\right)\middle|L^-\middle|d\left(yz,zx\right)\right\rangle$

Increase damping with increasing EF

Second order perturbation of SOI

D. Wang, et al., PRB **47**, 14932 (1993).

$$E_{\mathrm{PMA}} \propto (\xi)^2 \sum_{o,u,k} \frac{\left|\left\langle o,k,\downarrow\middle|L_z\middle|u,k,\downarrow\right\rangle\right|^2-\left|\left\langle o,k,\downarrow\middle|L_x\middle|u,k,\downarrow\right\rangle\right|^2}{\varepsilon_{u,k}^{\downarrow}-\varepsilon_{o,k}^{\downarrow}}$$

$$L_x=\tfrac{1}{2}\left(L^-+L^+\right)$$

The $\langle d(x^2\text{-}y^2)|L^-|d(yz)\rangle$ increase the damping, but decrease the PMA.⇒opposite EF dependence

Summary of the Third topic

First principles study on voltage control of magnetic anisotropy (VCMA) and magnetic damping in Fe/MgO interface

・For Fe/MgO(001) surface, the magnetic damping increases with increasing the electron accumulation at interface (positive EF).

(20% of damping constant α can be changed by EF=1[V/nm] for Fe/MgO(001))

・It is opposite to that of Perpendicular MCA.

・The voltage dependence of magnetic damping of Fe/MgO(001) can be attributed to the spin conservation term.

Summary of this talk

MRAM

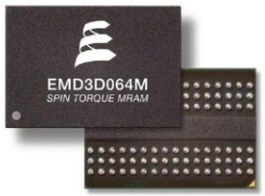

Magnetic sensor

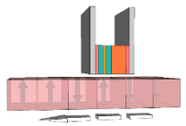

HDD read-out-head

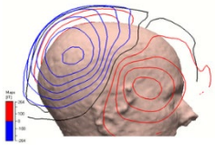

Earth's magnetic field sensor・current sensor for car・biomagnetic sensor

Corresponding to SQUID

Required performance for pMTJs

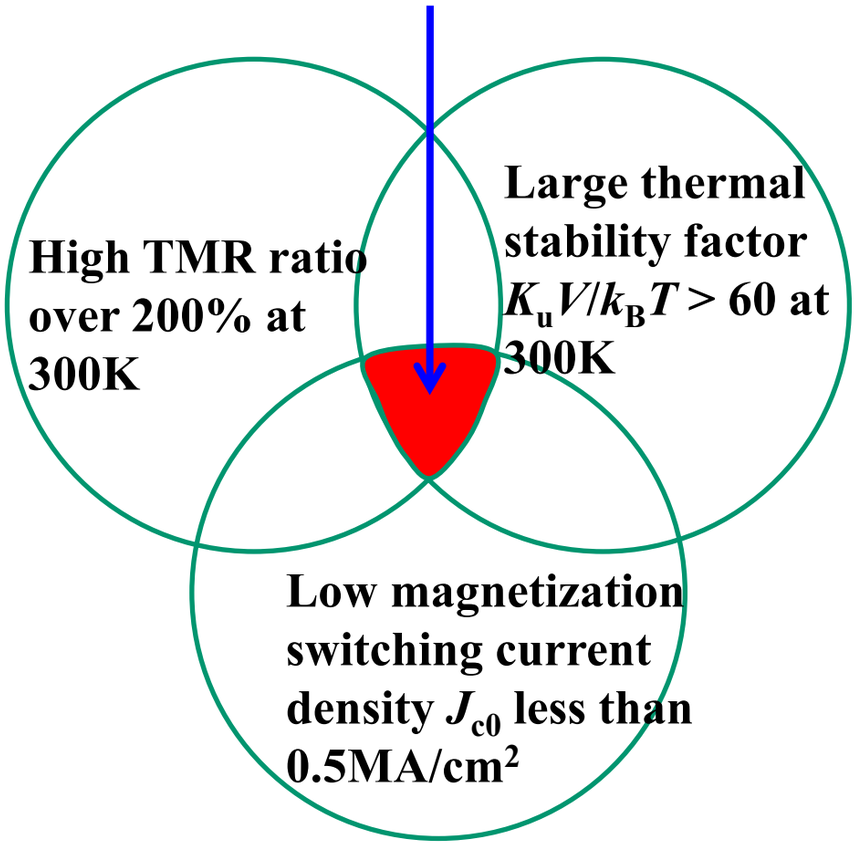

Required properties for spintronic materials

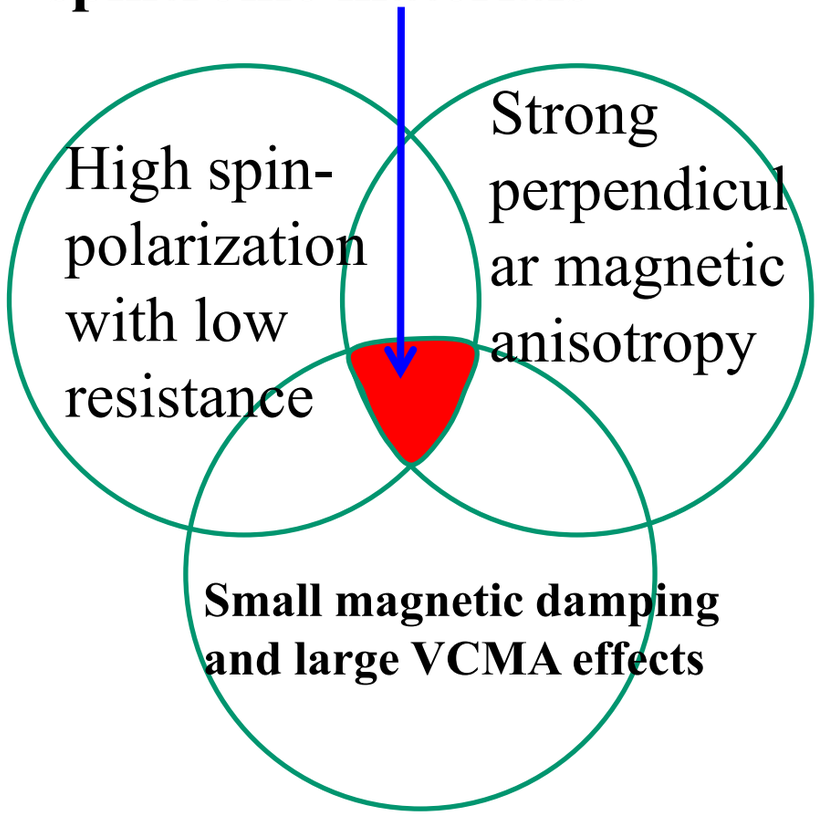

END